



## September 19, 2017 Puebla-Morelos Earthquake in Mexico Reconnaissance Report

The Canadian  
Association  
for Earthquake  
Engineering



L'Association  
Canadienne  
du Génie  
Parasismique

## **INTRODUCTION**

A magnitude 7.1 earthquake occurred in central Mexico on September 19, 2017 at 1:14 pm local time, causing widespread geotechnical and structural damage in the states of Morelos and Puebla, including parts of Mexico City, resulting in 369 casualties. The epicentre of the quake was 120 km southeast of Mexico City, 12 km southeast of the city of Axochiapan, Morelos on the boundary between Puebla and Guerrero. It occurred only 11 days after the  $M_w$  8.2 September 8, 2017 Mexico Earthquake, located further southeast, offshore Chiapas, Mexico. The September 19 event coincided with the 32<sup>nd</sup> anniversary of the tragic  $M_w$  8.0 Michoacan earthquake of 1985, reported to have resulted in over 9,500 deaths and 30,000 injuries (see Table 1). The Canadian Association for Earthquake Engineering sent a team of geotechnical and structural engineers to investigate the effects of the earthquake from Canadian seismic design perspective. The team conducted its investigation between October 15 and 23, 2017, during which period they also met with their colleagues at the National Autonomous University of Mexico (UNAM) and the Centre responsible for the Mexican earthquake early warning system, the Centro de Instrumentación y Registro Sísmico (CIRES) and gathered valuable background information. This report provides a summary of the team's findings.

The CAEE team and their specializations are listed below in alphabetical order:

- Carlos Cruz, University of Alberta, Edmonton, AB (Building Structures)
- Sharlie Huffman, Huffman Engineering, Victoria, BC (Bridge Structures)
- David Lau, Carleton University, Ottawa, ON (Bridge Structures)
- Robert Lo, Klohn, Crippen, Berger, Vancouver, BC (Geotechnical Engineering)
- Murat Saatcioglu, University of Ottawa, Ottawa, ON (Building Structures)
- Odin Guzman Sanchez, University of Alberta, Edmonton, AB (Building Structures)
- Samuel Yniesta, Ecole Polytechnique, Montreal, QC (Geotechnical Engineering)

This CAEE report focuses on the observations made by the team during its visit (see also Saatcioglu et al. 2019 and Lo and Yniesta 2019, respectively, for a summary version of the structure and geoscience aspect). Readers are referred to a comprehensive Geotechnical Extreme Events Reconnaissance Report (GEER 2018) sponsored by the US National Science Foundation for general background and detailed documentation of their work. Additional references by the host country (II.UNAM 2017b), USA (SEAOSC 2017, Galvis et al. 2017, Post 2017), and Japan (Alberto et al. 2017) are listed in the references at the end.

## **GEOSCIENCE ASPECTS**

### **Mexico City seismo-tectonic setting**

The bulk of Mexico is located over two large tectonic plates: North America and Cocos plates. This is one of the world's most active seismic regions (see Benz et al. 2011, and Fig. 1). The Cocos plate moves northeastward and subducts under the North America plate along the Middle America trench. The rate of plate convergence in the area ranges from 63 to 76 mm per year. Due to this convergence, the Mexican land mass is crumpled to form the Cordillera Neovolcánica mountain ranges of southern Mexico. As the

Cocos plate subducts, it melts. The molten material is forced upward through fractures in the overlying North America plate. The process has caused frequent earthquakes and occasional volcanic eruptions.

**Table 1. Comparison of Earthquake and Damage Data – September 19, 1985<sup>1</sup> vs 2017<sup>2</sup> Earthquakes**

| Date<br>(Local Time)      | Earthquake Location | Type       | Focal Mechanism                  | Peak Acceleration Intensity, MMI   | Special Features  | Casualties   | Damages  |  | General References                        |
|---------------------------|---------------------|------------|----------------------------------|--|---|--|--|--|---|
|                           |                     |            |                                  |  |   |  | General  | Lifelines  |   |
| 1985 Sep 19<br>(7:17:47)  | Michoacan, Mexico   | Interplate | Mw 8.0, Depth 27.9 km Thrust eq. | In general, MMI up to VII in coastal area, and up to VI in Mexico City, but in localized zones MMI up to VIII- IX in coastal area, and up to IX-X at mouth of Balsas River, and up to VIII-IX in Mexico City | The event caused significant improvement of building codes in Mexico as well as many other countries including Canada and USA               | Very High death ~9,500+ injured ~30,000 displaced >100,000         | Cost of damage ~3 to 4 billion US dollars, 412 buildings collapsed and 3,124 buildings seriously damaged in Mexico City. | Damage and collapse of SCT Communications building, (causing disruption of long-distance telecommunication over 3 weeks) and several medical facilities and school buildings | USGS <sup>1</sup><br>Mitchell et al. 1986 |
| 2017 Sep 19<br>(13:14:38) | Puebla, Mexico      | Intraplate | Mw 7.1, Depth 48 km Normal eq.   | Up to VI – VII in Mexico City  | Ground cracks causing significant damages in buildings, roads, water/sewer lines in Colonia Del Mar and Cienega San Gregorio of Mexico City | Low death: ~220+ in Mexico City 142 in other cities injured ~6,000 | 44+ buildings collapsed, many others damaged in Mexico City, many collapsed and damaged buildings in other cities        | Significant damages in electric grid, water and sewer lines (particularly in Colonia Del Mar) of Mexico City, some collapsed and damaged bridges in other cities             | USGS <sup>2</sup><br>GEER 2018            |

Notes: 1. <https://earthquake.usgs.gov/earthquakes/eventpage/usp0002jwe/executive>

2. <https://earthquake.usgs.gov/earthquakes/eventpage/us2000ar20/executive>

Mexico has a long history of destructive earthquakes and volcanic eruptions. In September 1985, a magnitude  $M_w$ 8.0 earthquake killed more than 9,500 people in Mexico City. Seismic events affecting Mexico City include: crustal events within the upper North America plate (Suter et al. 1996), intraplate events within the lower Cocos plate (Singh et al. 2015, 1999, 1997, 1996) and the interplate events at the interface between the two plates (Singh 1985).

In southern Mexico, Volcán de Colima and El Chichón erupted in 2005 and 1982, respectively. Parícutín volcano, west of Mexico City, began venting smoke in a cornfield in 1943; a decade later this new volcano had grown to a height of 424 meters. Popocatepetl and Ixtaccíhuatl volcanos ("smoking mountain" and "white lady," respectively), southeast of Mexico City, occasionally vent gas that can be clearly seen from the City, a reminder that volcanic activity is ongoing. From 2004 to 2018 (ongoing) Popocatepetl renewed its activity forcing the evacuation of nearby towns, causing seismologists and government officials to be concerned about the potential effect of a large-scale eruption might have on the heavily populated region.



Fig. 1 Cocos Plate Subduction zone. Credits: (Graphic) G. Grullón, and V. Kostoglodov

### **Characteristics of Two Intraplate Earthquakes Occurred in September 2017**

The magnitude 8.2 earthquake of September 8, 2017 occurred offshore Chiapas, Mexico, as the result of normal faulting at a depth of 47.4 km. It involved a rupture plane of about 200 km long and 50 km wide. Over the preceding century, the region within 250 km of the hypocentre has experienced 8 other M 7+ earthquakes. Most occurred in the subduction zone to the southeast of this event, near the Mexico-Guatemala border, and none were larger than M 7.5. The largest event was M 7.4 thrust faulting earthquake offshore Guatemala in November 2012, resulted in at least 48 fatalities and over 150 injuries, and significant damage near the coast.

The magnitude 7.1 earthquake of September 19, 2017 was also a normal faulting intraplate event at a depth of approximately 48 km (USGS 2018b). It involved a rupture plane of about 50 km long and 20 km wide. Over the preceding century, the region within 250 km of the hypocentre experienced 19 other M 6.5+ earthquakes. Most occurred near the subduction zone interface at the Pacific coast, to the south of the September 19 event. The largest was a M 7.6 earthquake of July 1957 in the Guerrero region with 50 to 160 fatalities and many more injuries. This event was followed by a M 7.0 quake at 70 km depth, just to the southeast of the September 19, 2017 earthquake, which caused 14 fatalities, about 200 injuries, and considerable damage in the city of Puebla.

The above two intraplate events remind us that this type of earthquakes also poses significant threat to the Mexico City, because they could come from the south in a wide range of directions with shorter epicentral distances and occur more frequently than the large-magnitude interplate events along the Pacific coast (see Fig. 1).

Canadian west coast shares a similar seismo-tectonic setting as the southern Mexico region with the subduction of the Pacific Ocean plate and smaller Explore and Juan de Fuca oceanic plates along the Cascadia fault under the overlying North American continental plate. The plate convergence rate near Victoria/Vancouver is 40 mm per year, about half of that in the southeastern Mexico region. This similarity has influenced consideration of seismic hazard in the Canadian west coast since the 1985 Michoacan Mexico Earthquake (Atkinson and Adams 2013).

### **Lacustrine sediments in the Mexico City basin**

Central Mexico is vulnerable to seismic hazard due to its seismo-tectonic setting. As a major metropolitan centre with a large population, Mexico City poses additional seismic hazard because of its subsoil profile including thick, soft lake deposits. The widespread presence of lacustrine deposits in the Valley of Mexico basin, including Mexico City, dictates the foundation problems encountered by structures in the city. These problems include regional ground subsidence and differential settlement of buildings. During seismic events, the relatively soft lacustrine deposits tend to amplify ground motions, increase site natural periods and lengthen the duration of shaking. While the problem of ongoing ground subsidence due to extraction of groundwater in the Mexico City is widely recognized for decades, the somewhat related problem of ongoing ground cracking and its intensification during seismic events, such as the September 19, 2017 event, has only recently been studied systematically since 2005. II.UNAM (2017a) provides a comprehensive background of this unique subsoil issue covering the city's development over a period of

six decades from 1959 to 2016. The GEER Report (2018) also summarizes the seismic aspects of this type of soil condition succinctly.

## **Early-Warning system**

### *Historical development of the early warning system*

The 1985 Mw8.0 earthquake was an interplate subduction event, which originated from the rupture of a segment of the Cocos plate subduction zone known as the Michoacan gap, northeast of the Guerrero Gap (see Fig. 1). This subduction zone is particularly active and has generated 42 earthquakes of magnitude 7 or greater in the last century (Anderson et al. 1986). The September 8th, 2017 (UTC time) Mw8.2 earthquake originated from the southern end of the subduction zone near the Tehuantepec Gap. The Guerrero gap remains a major seismic threat as it has not ruptured since the beginning of the 20th century.

After the deadly 1985 earthquake, the Mexican authorities established the law for Civil Protection to mitigate the consequence of future earthquakes. Since 1987, the authorities have promoted the creation of an early warning system with the aim of reducing human loss in future earthquakes. The principle of the early warning system is to detect large earthquakes recorded by strong motion accelerometers, and to send an alert to the main population centres when such an earthquake is detected. The main immediate concern for the authorities was an interplate earthquake originating from the Guerrero gap, a zone situated 320 km from the Mexico City and capable of causing major destruction (García-Acosta and Suárez 1996). This concern led the Mexico City Authorities to create the Sistema de Alerta Sísmica Mexicano (SASMEX) in 1991. Thereafter this effort was led by the Centro de Instrumentación y Registro Sísmico (CIRES). One of its responsibilities is to operate and maintain the network of recording stations. Initially only 12 stations were established as compared to more than 90 stations now in operation. The system began operational in 1991, and has been available to public since 1993.

Since the main concern was an earthquake originating from the interplate zone, the sensors were installed on the western coast as priority. While this is advantageous for early detection of large interplate earthquakes, it is less effective for detection of intraplate earthquakes which tend to occur further inland.

### *Operating principles of the system*

When an earthquake is detected at a recording station, the system automatically estimates the magnitude of the earthquake based on an algorithm that correlates empirically the magnitude and the time of arrival of the P-waves. When the time of arrival of S-waves is determined, a different correlation is used to get a new estimate of the magnitude. A third correlation uses the time lapse between the arrivals of the P and S-waves to define the magnitude.

When a large earthquake is detected at one station, the system does not send an alert yet, rather it waits until the earthquake is detected by a second station. If the two magnitude estimates are inconsistent, the system remains silent and waits for confirmation from detection at a third station. The expected magnitude is always re-evaluated when a new station detects the earthquake. Since P-waves travel faster than S-waves, they are detected first. P-waves can be detected at a second station before the S-waves arrive at the first. In such a case an alert can be triggered without any information on the S waves. Only earthquakes

with a magnitude greater than 5 can trigger an alert. Population centres situated too far from the epicenter to receive significant shaking will not receive an alert.

Alerts are sent through a network of very high-frequency communication stations which can issue warning in two seconds or less (Cuéllar et al. 2014). In Mexico City, about 8,200 speakers are installed and emit an alarm when an earthquake is detected. In addition to speakers, alerts are also broadcasted on TV and radio. The CIRES also installs alert systems in buildings. Most of public schools are equipped with such a system along with fire stations and hospitals. The Mexico City Metro also receives SASMEX alerts, although they are used to stop trains, and not to warn commuters.

Performance of the early-warning system during the September 19th, 2017 Puebla - Mexico City earthquake

The intraplate 7.1 earthquake was first picked up by recording stations situated in the Puebla state. For this earthquake, all major population centres, except Morelia, were warned (see Fig. 2). Given the short distance to the epicentre, Mexico City was only given 20 seconds of warning before strong shaking occurred. The fact that only a few recording stations were situated around the epicentral area contributed to relatively short warning time. In fact, when the alarm went off in Mexico City, the low amplitude P-wave had already been felt. The warning siren also tended to be masked somewhat by the cacophony of urban noise. However, the successful execution of the early-warning system attests the due diligence of the agency in charge as well as the opportunities of frequent seismic events available to root out system shortcomings.

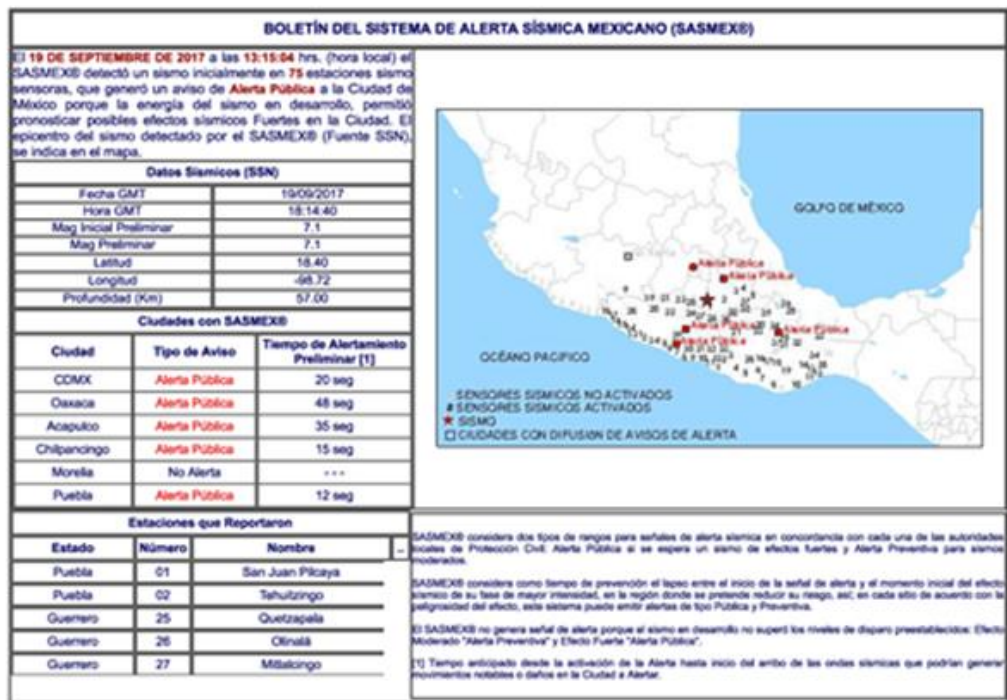


Fig. 2 Screenshot of the CIRES website summarizing the alerts sent on September 19th, 2017

## Ground motions and site effects

### Subsoil zonation

The 1976 Mexican building code initially defined 3 seismic zones for Mexico City: the hill zone (Zone I), the transition zone (Zone II), and the lake zone (Zone III). The zones are defined based on the fundamental site period, which is essentially a function of the thickness of soft lacustrine clay. The latest version of the building code (NTCS-04 2004) further divides Zone III into 4 sub-zones (IIIa, IIIb, IIIc, and IIId) as shown in Figs. 3 and 4. Throughout Mexico City, the thickness of lacustrine clay varies from 0 m in the hill zone (Zone I) to about 60 m in Zone IIId with the fundamental site period varying from about 0.4 sec to 4 sec.

### Geographical distribution of damaged buildings

The Colegio de Ingenieros Civiles de México (CICM) website [www.sismosmexico.org](http://www.sismosmexico.org) presents the geographical distribution of building damages in Mexico City, as shown in Figs. 3 and 4. Damaged buildings shown by the red symbols in Fig. 3 are deemed unsafe for occupation following the September 19<sup>th</sup> earthquake, while those shown by the black symbols in Fig. 4 represent collapsed buildings. The majority of collapsed and damaged buildings are located in the western portion of the transition zone (Zone II), and the two lake subzones with smaller clay thickness (Zone IIIa and IIIb). It is interesting to note that only a handful of buildings in Zone IIId, where the lacustrine clay thickness is greatest, were damaged and none of them collapsed.

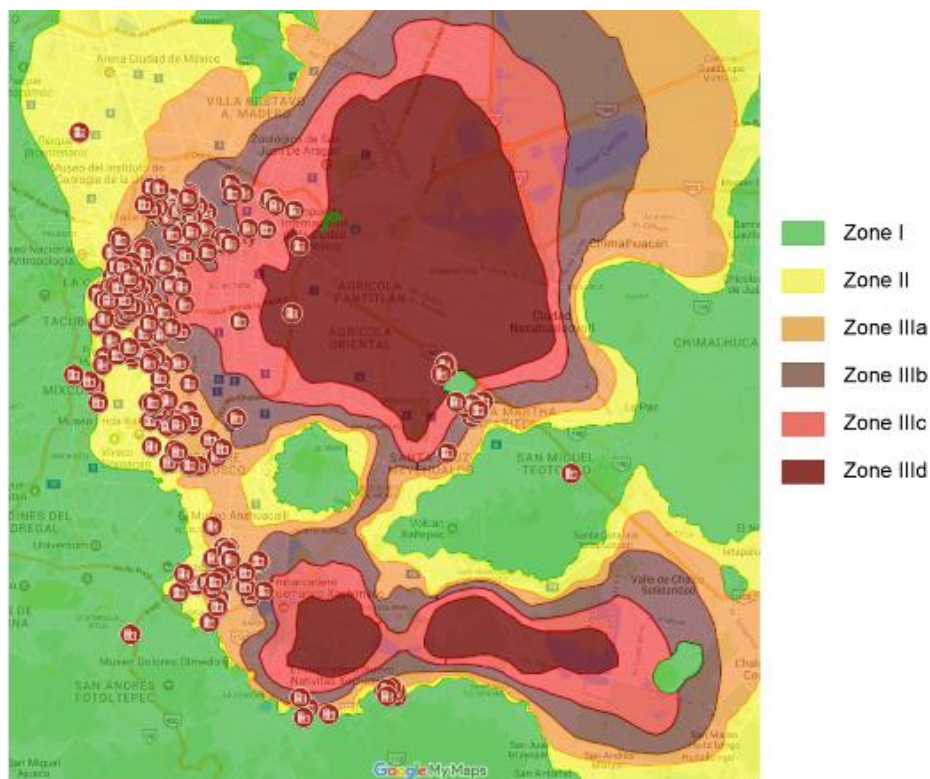


Fig. 3 Map showing buildings deemed unsafe for occupation <https://www.sismosmexico.org/mapas>

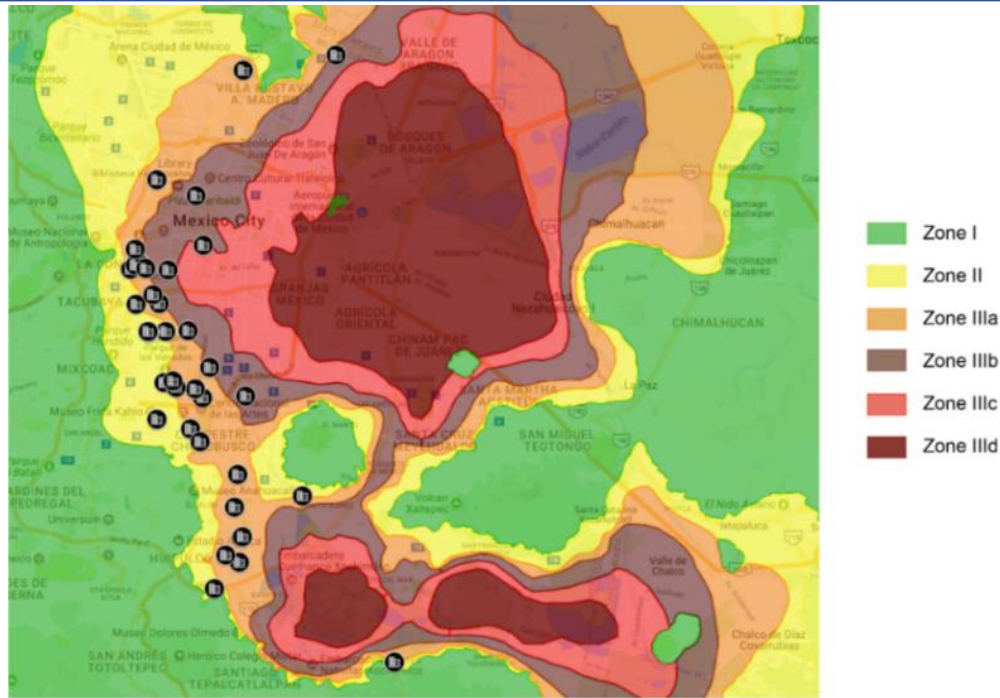


Fig. 4 Map showing collapsed buildings <https://www.sismosmexico.org/mapas>

#### Ground motion recordings

Raw earthquake recordings were provided by the Centro de Instrumentacion y Registro Sismico (CIRES, [cires.org.mx](http://cires.org.mx)). A total of 61 records were retrieved from the recording stations located in six seismic zones in Mexico City (see Fig 5). Table 2 presents the average properties of these stations in each seismic zone. The raw earthquake recordings were filtered by Yniesta (2019) in order to calculate acceleration, velocity and displacement response spectra for all three components of ground motion. Results of Yniesta's ground response analysis show that the highest peak ground acceleration (PGA) was observed in Zone IIIa, where it was about twice the PGA value observed in Zone I. PGA values in other zones (Zone II, Zone IIIb to IIIc) are roughly comparable. The higher accelerations found in Zone II and Zone III were confirmed by the shake map shown in Fig. 6. Peak ground velocity (PGV) and peak ground displacement (PGD) values increased with the increase of zone softness.

Table 2 Ground motion recording stations average properties

| Zone | Average $V_s$ (m/s) | Average Site Period $T_s$ (s) | Number of recording stations |
|------|---------------------|-------------------------------|------------------------------|
| I    | 117.4               | 0.43                          | 7                            |
| II   | 115.1               | 0.52                          | 9                            |
| IIIa | 94.2                | 1.05                          | 8                            |
| IIIb | 82.8                | 1.73                          | 15                           |
| IIIc | 81.8                | 1.96                          | 12                           |
| IIIc | 81.8                | 2.26                          | 10                           |

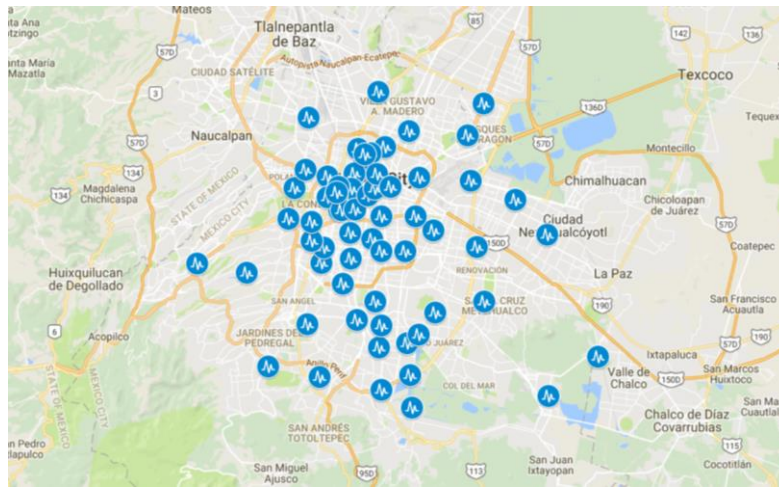


Fig. 5 Location of recording stations <https://www.sismosmexico.org/mapas>

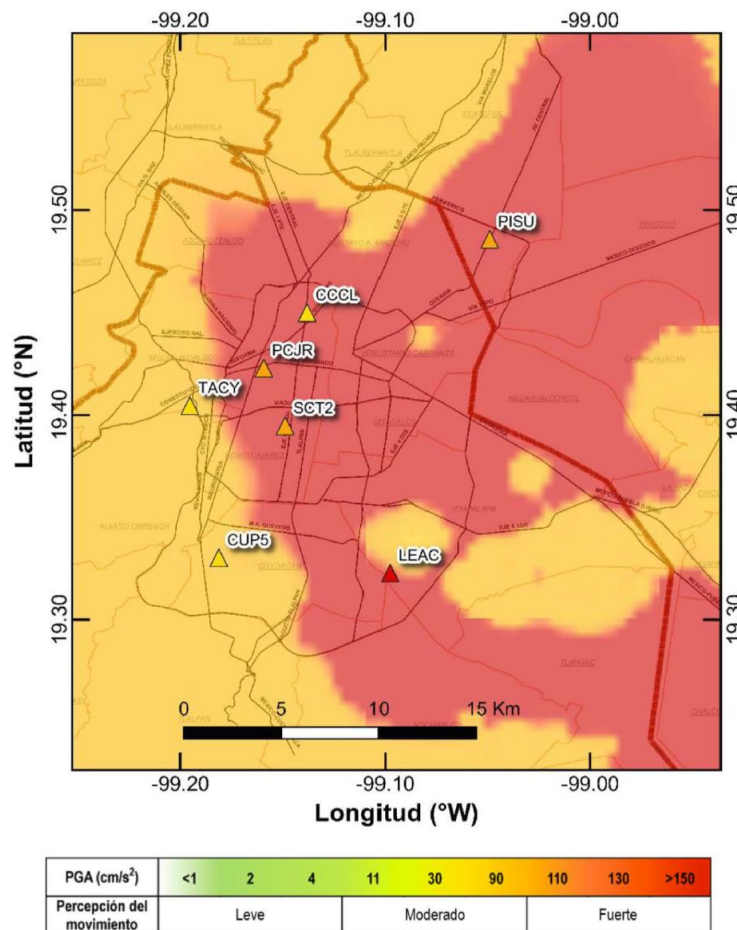


Fig. 6 Map of PGA (cm/s<sup>2</sup>) during the September 19th Earthquake (from IINGEN 2017)

Fig. 7 presents selected response spectra for each zone. The selected spectra are representative of the average spectra observed over a given zone, except Fig. 7(a) for the hill zone (I). (Note: The spectra in

Fig. 7(a) is larger than the average spectra in the hill zone.) One of the takeaways from Fig. 7 is that the frequency content of the motion spectrum changes when going through zones of increasing softness. The larger spectral response is observed at greater periods in the softer zone, which is to be expected. However, the spectral acceleration for these zones is relatively low. Note that the frequency content of the vertical acceleration spectra is essentially independent of the softness of the zone, in part because it is relatively low. The elongation of spectral mean period and the large response observed in Zone II (and IIIa to a lesser extent) is due to the effect of soil response on the propagation of seismic waves.

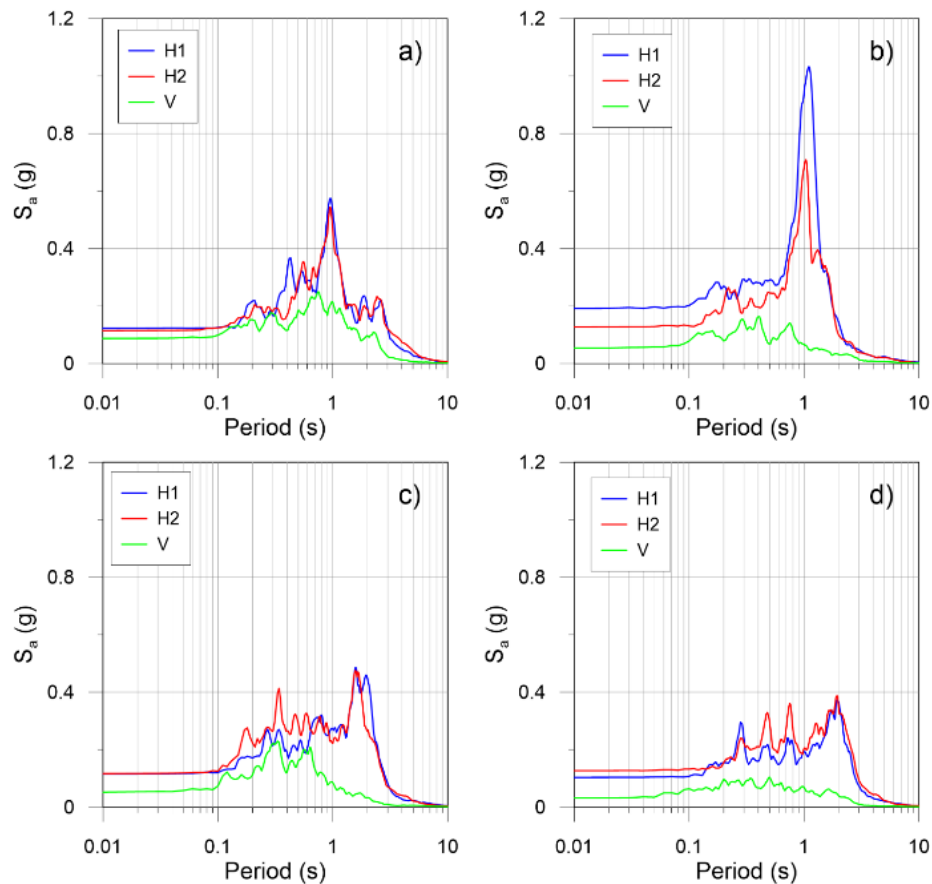


Fig. 7 Acceleration response spectra (5% damped) at recording station: a) MY19 (Hill zone I)  
b) DX37 (Transition zone II), c) CI05 (lake zone IIIa) and d) PE10 (Lake zone IIIb)

### Ground motion amplification due to site subsoil conditions

#### *Dynamic soil properties of the soft lacustrine clay*

The soft lacustrine clay in Mexico City is situated on the location of the former Texcoco lake. The shallower soil strata are composed of soft, high-plasticity lacustrine clay. This soft clay has been found to be prone to amplify seismic motions (Mayoral et al. 2016) because of its low shear wave velocity (64 m/s) and relatively linear modulus reduction curve. The reduction in shear modulus, as well as increase in soil damping is relatively moderate for strains of up to 0.1% (see Fig. 8). Previous studies have found that nonlinear soil response is generally absent during seismic ground motion (Ordaz and Singh 1992). Arroyo

et al. (2013) have concluded that soft lacustrine sediments of Mexico City tend to amplify ground motion over a broad period range between 1.0 and 5.0 sec.

### Ground motion amplification

Ground motion amplification is a complex process, which depends on soil stratigraphy, stiffness, nonlinear response, as well as the intensity and frequency content of the input motion. Three-dimensional effects also come into play. In general, ground motion amplification due to soil effect is studied through the vertical propagation of horizontal shear waves. In this section, the reference ground motion is taken as the average motion observed in the recording stations situated in the hill zone (Zone I), since this is the stiffest zone. Ground motion amplification observed in Zones II and IIIa can be explained by the frequency content of the input motion.

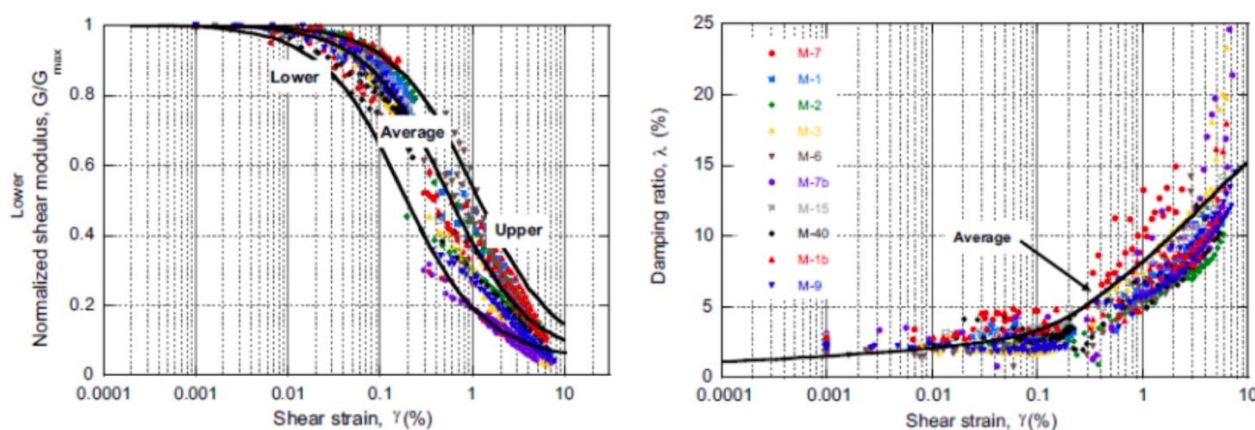


Fig. 8 Modulus reduction and damping curves for the lacustrine soft clay (Mayoral et al. 2016)

The shift in frequency content at all sites is consistent with the response spectra presented in Fig. 7. The frequency content of the response spectra is of interest because it defines the motion transmitted to the buildings located on the subsoil. Most of the buildings that collapsed were 7-10 storey high, and were associated with a fundamental period of about 1.0 sec. The motions in Zones II and IIIa had predominant spectral period of about 1.0 sec, and had the highest spectral acceleration, which would affect specifically this type of buildings. Figure 9 presents the shake map for spectral acceleration at 1.0 sec, and the shake map confirms that the maximum spectral acceleration at 1.0 sec was observed mostly in the transition zone where building damage and collapse were seen.

### Change in site period due to regional subsidence

Because of regional subsidence, the thickness of soil layers in Mexico City has reduced at a much higher rate unseen in other cities. As the soft subsoils consolidate, their shear wave velocities increase. Arroyo et al. (2013) studied the potential decrease of site period with time due to subsidence. They established a simplified stratigraphy, depicted in Fig. 10, and created a model to calculate the evolution of site period with ongoing subsidence caused by the lowering of groundwater table. Figure 11 shows the predicted evolution of site period at the recording station PE10 situated in the lake zone (III d) for which response spectra for the September 19<sup>th</sup> Earthquake was presented in Fig. 7(d). A decrease in site period at the lake

zone would mean that the ground motion amplification would occur at a shorter period. In other words, in the future, an event similar to the September 19<sup>th</sup>, 2017 Earthquake would induce more damage in the lake zone than in the September 2017 event. This effect is illustrated in Fig. 12, which presents the amplification factor as a function of the period during two different seismic events at station PE10. The peak amplification occurred at a shorter period in the more recent event of 2007 than in the major event of 1985.

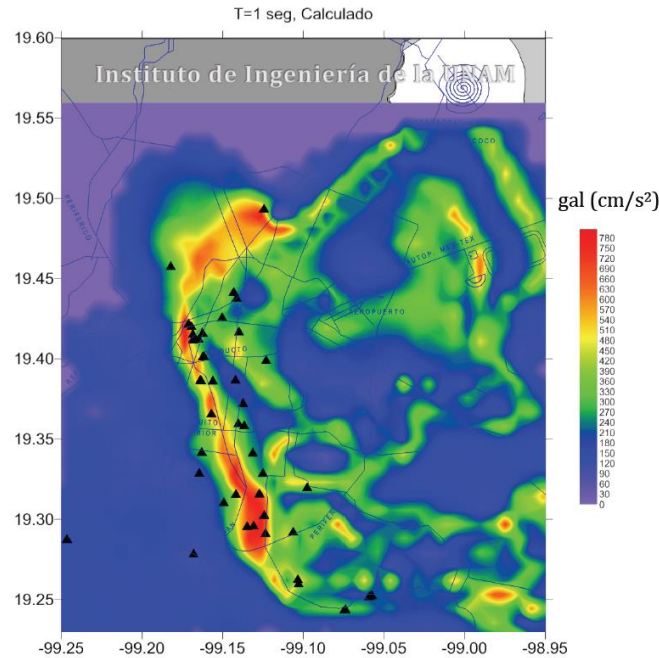


Fig. 9 Shakemap for spectral period of 1.0 s representative of 7 to 10-storey buildings (from the Grupos de Sismología e Ingeniería de la UNAM 2017)

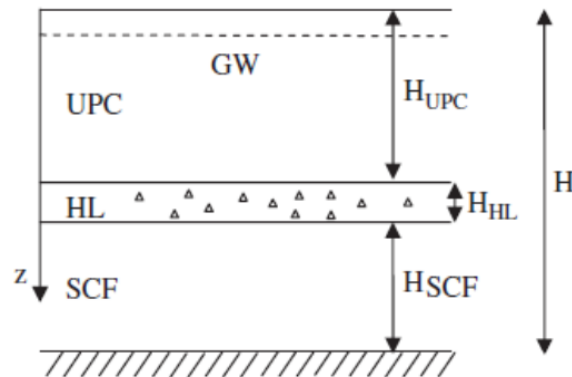


Fig. 10 Typical soil profile considered in Arroyo et al. 2013

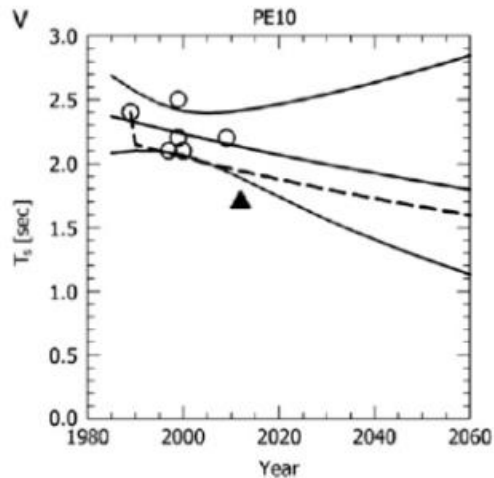


Fig. 11 Change of site period with time at recording station PE10 (zone IIIId) from Arroyo et al. (2013)

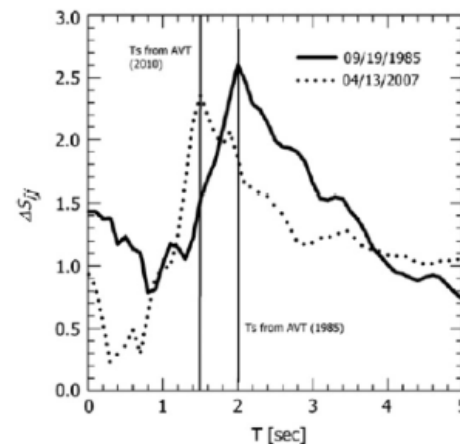


Fig. 12 Effect of site period changes with time (Arroyo et al. 2013)

### Other potential site effects

Additional factors influencing site effects include basin effect and topographic effect. Basin effect is different from that described in the preceding section. It arises from the reflection and refraction of trapped inclined shear waves in a sedimentary basin rather than from soil nonlinearity and impedance contrast. Topographic effect defines ground motion amplification at topographic features due to seismic waves focusing. These two effects have long been recognized as major sources of potential local ground motion amplification, and are acknowledged here that they need to be considered in a more thorough study.

## **FOUNDATION ASPECTS AND GROUND FAILURES IN MEXICO CITY**

### **Subsoil condition**

Mexico City is located in the Valley of Mexico, which before the completion of the Nochistongo drainage cut in 1789 was a closed basin containing numerous lakes. These lakes have been partially filled by alluvium and clay derived from weathered volcanic rocks (Marsal and Mazari 1969; Marsal 1975). The original city is built on the location of the old Aztec capital Tenochtitlan, see Fig. 13(c), which was established on an island in Lake Texcoco with three causeways connected to adjacent lands. As Mexico City grew it expanded from the old island, across the former lakebed, and onto the surrounding hills. As reported by Marsal (1975), the upper and lower clay layers have water contents of about 300% and 200% and unconfined compressive strengths of about 80 kPa and 150 kPa, respectively. The first competent (clayey sand) layer has an unconfined compressive strength of 230 kPa. Geotechnical problems associated with Mexico City clay are regional subsidence (up to 9 m) due to groundwater withdrawal, building settlement (total and/or differential settlement), subsoil disturbance due to adjacent foundation construction, and severe earthquake shaking. Figure 13(a) shows the current map of geotechnical seismic zoning for Mexico City, where Zone III is further sub-divided into four sub-zones: from Zone IIIa to Zone IIIId based on clay thickness (see Figs. 3 and 4 as presented and discussed earlier). Figure 14 shows typical subsoil profiles for Zone III.

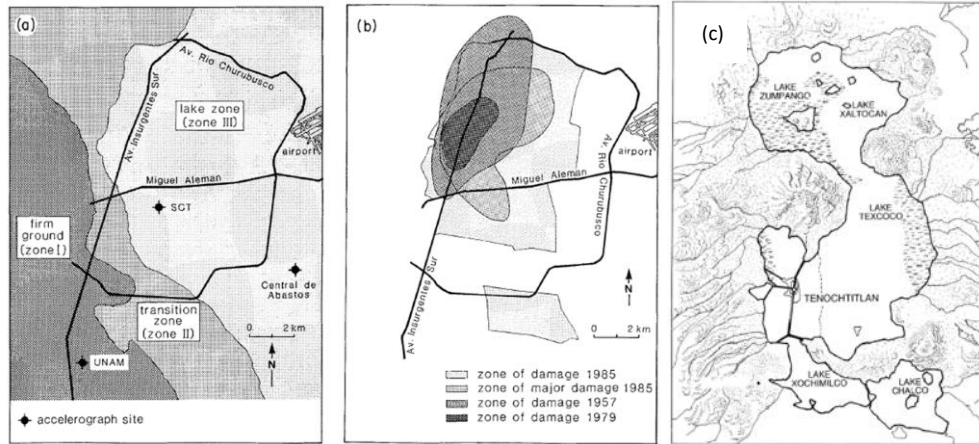


Fig. 13(a) Subsoil zones of Mexico City, (b) damage zones in the 1957, 1979, and 1985 earthquakes and (c) City of Tenochtitlan (modified from Mitchell et al. 1986 and Sabloff 1997)

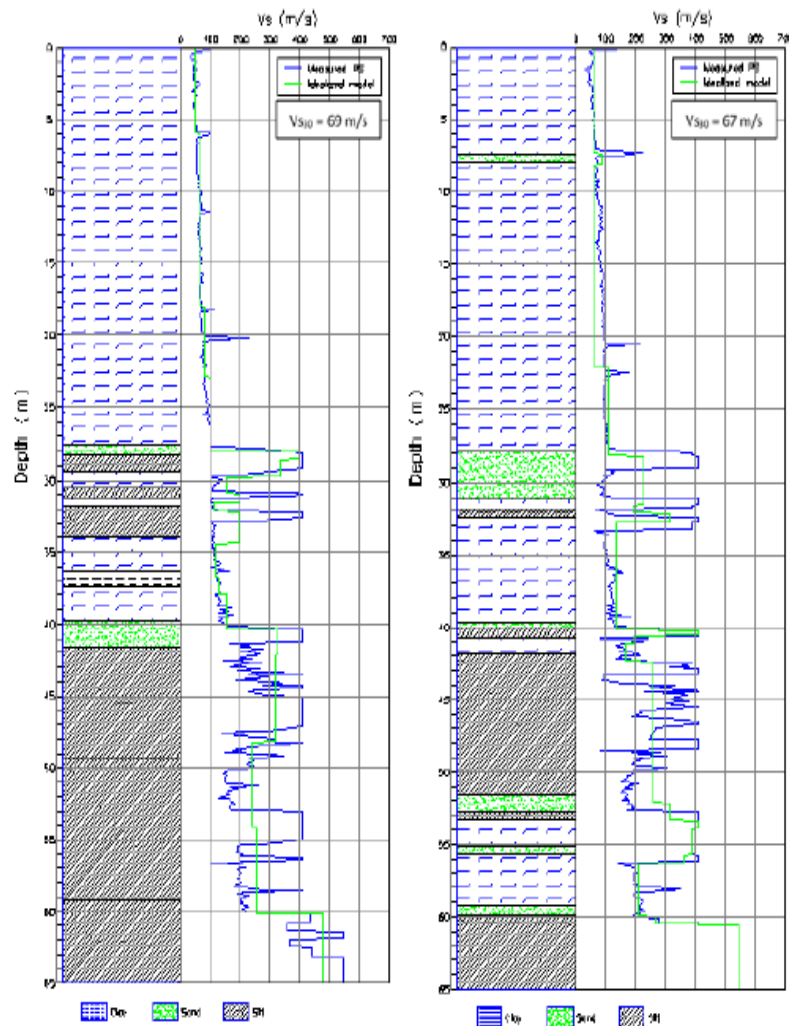


Fig. 14. Typical subsoil profiles for Zone III (Mayoral et al., 2016)

### Foundation practice

Different types of foundations typically used in Mexico City are illustrated in Fig. 15. Light structures are usually founded on shallow footings of masonry or concrete, Fig 15(a), that are sometimes interconnected by grade beams. In order to mitigate settlement problems for larger structures, "floating" or, technically more correct, "compensating" rigid-box foundations are used to compensate for the building weight as illustrated in Fig. 15(b). End-bearing piles, Fig. 15(c), are used for heavier structures. This, however, could cause the ground floor to be above grade as the surrounding ground settles with time. Friction piles, Fig. 15(d), tend to mitigate this problem, because the piles settle with the supporting soil. Interlaced piles, depicted in Fig.15(f) stiffen the supporting soil and therefore exhibits a behaviour somewhere in between that of end-bearing and friction piles. End-bearing control piles, shown in Fig. 15(e) transfer the building weight through compressible cushions having chosen load-deformation characteristics that would permit the structure to follow the ground settlements in a controlled manner. Figure 16 shows the photo of such an installation, which would require periodical adjustments of the control elements to harmonize settlement of the structure with that of the surrounding ground. The famous Latin American Tower (La Torre Latinoamericana) has both end-bearing piles and a "compensating" foundation, designed by Zeevaert (1956, 1982). The tower performed very well during both the 1985 Mw8.0 and the 2017 Mw7.1 earthquake. Many buildings in Mexico City become tilted due to differential settlement caused by static and/or seismic loading. Valenzuela-Beltrán et al. (2017) looked into additional strength requirement for asymmetric yielding of this type of buildings, and

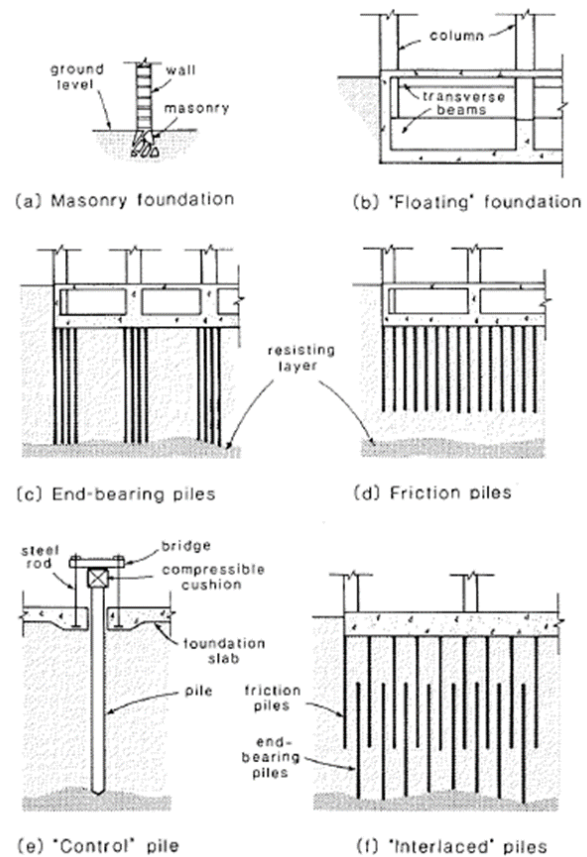


Fig. 15 Foundation types used in Mexico City (from Mitchell et al. 1986 and Marsal 1975)



Fig. 16 End-bearing control piles supporting the La Plaza Condesa building (GEER 2018)

recommended code-related provisions for their seismic design.

### Ground deformation and failure

Extensive ground failures were observed in different regions. The GEER (2018) report provides a detailed discussion of ground deformation and failures caused by the September 19, 2017 Earthquake. The observations made by the CAEE team are presented in the following sections, identified by site locations. They include: slope instability (Site 1), ground cracking and settlement (Sites 2 and 3), causeway lateral-spread (Site 4) and canal masonry wall slump (Site 5).

#### *Site 1: Slope Instability, Xochimilco*

Slope instability was observed at Xochimilco in a residential area located on a hill slope. Anecdotal evidence indicated that the slope had deformed prior to the earthquake probably due to groundwater withdrawal by pumping, and the deformation became more substantial after the quake. Aerial view of the slope instability with marked cracks is shown in Fig. 17 (GEER 2018). The deformed hill slope consists of roads at three levels: the base, 1<sup>st</sup> and 2<sup>nd</sup> level; one drill rig was set at each of the two lower levels as shown in Figs. 18(a) and 18(b). The main crack was along the 1<sup>st</sup> level road, while a shorter crack was on the 2<sup>nd</sup> level road as can be seen in Figs. 19(a) and 20(a). The damaged masonry wall on the 1<sup>st</sup> level road was being repaired at the time of our visit, with new masonry materials transported in and stockpiled on the road, and a short distant end-segment of the deformed wall was shored up by timber struts. Houses on the hill slope above the 2<sup>nd</sup> level road appeared to be in good condition, with minor masonry debris on the road side.



Fig. 17 Aerial view of the Xochimilco slope instability with marked cracks and pipeline breaks  
(GEER 2018)



(a)



(b)

Fig. 18 Drill rig sets on road side - (a) road at hill base, (b) the 1<sup>st</sup>-level road



(a)



(b)

Fig. 19 (a) Longitudinal crack on the 1<sup>st</sup>-level road (b) damaged masonry wall on the 1<sup>st</sup>-level road



(a)



(b)

Fig. 20 (a) Road condition on the 2<sup>nd</sup>-level road, (b) condition of houses above the 2<sup>nd</sup>-level road

### Ground Cracking and Settlement

The problem of ongoing ground cracking and its intensification during seismic events, such as the September 19, 2017 event, has only recently been studied systematically since 2005 (II.UNAM 2017a). Factors contributing to this phenomenon include: (1) hydraulic fracturing in flooded areas; (2) regional subsidence in areas with abrupt transition; (3) stratigraphic anomalies; (4) evapo-transpiration; and (5) buried geologic structures. Figure 21 shows the locations where soil fracturing has been reported in Mexico, including areas outside of Mexico City.

The suspected causes of ground cracking observed in Sites 2 and 3, discussed subsequently, are: regional subsidence in areas with abrupt subsoil transition, stratigraphic anomalies and buried geologic structures, although hydraulic fracturing and evapo-transpiration may also play some roles. The three former potential causes would be influenced by the following geotechnical and geological anomalies in the subsoil lake deposits (see Fig. 22 for distribution of these anomalies in seismic Zone II and III):

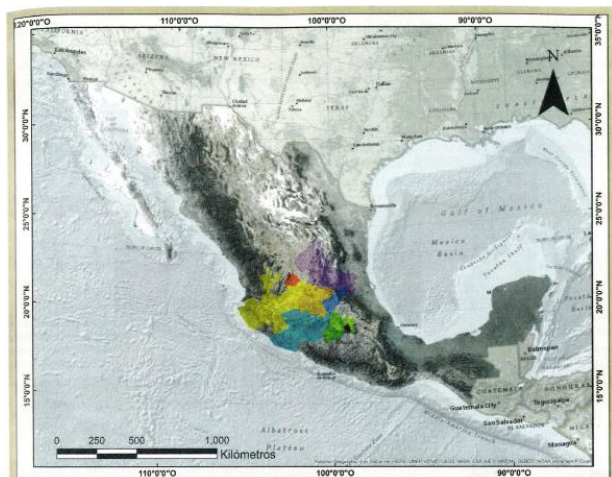


Fig. 21 Mexican states where ground cracking has occurred, shown in coloured patches

(from Auvinet et al. II.UNAM 2017a)

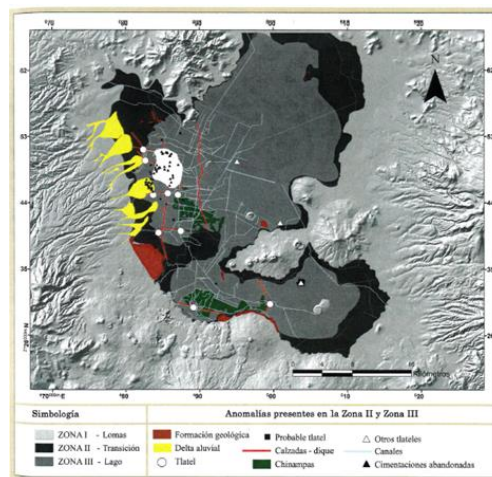


Fig. 22 Geotechnical anomalies in Seismic Zones II and III of Mexico City

(from Auvinet et al. II.UNAM 2017a)

#### Geotechnical anomalies:

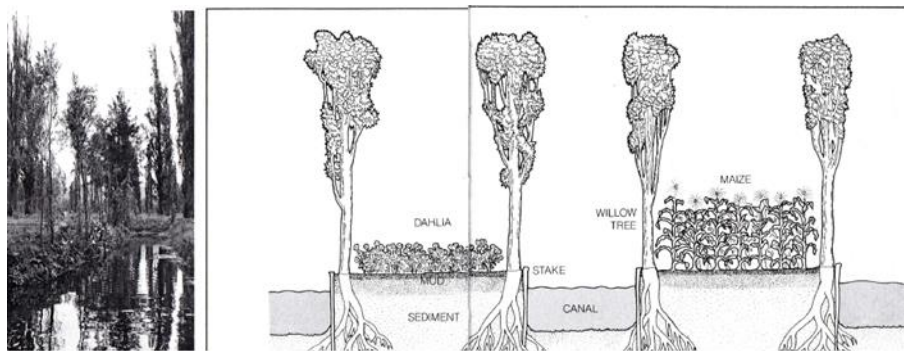
- Tlatels – “raised ground” derived from the “nahuatl” language;
- Causeways and dykes – constructed over time for transportation links and flood control;
- Chinampas or “floating gardens” (see Fig. 23 for illustrations) - constructed in shallow lakes for enlarging cultivated areas by reclaiming swamp lands;
- Canals – constructed for conveying runoff through the city “basin”.

#### Geological anomalies:

- Geomorphological feature related to rock mass, such as Turba o Loma de San Luis; and
- Solidified hard tuff layer from a recent volcanic event and subsequently embedded in the soft clay lake deposits in the vicinity of the Colonia del Mar in Tlahuac. The tuff layer undergoes rupturing process as the result of regional subsidence due to groundwater withdrawal by pumping.

The above anomalies, whether geotechnical or geological, provide physical settings that would involve abrupt transitions in subsoil profiles. Under static and/or seismic loading differential ground settlement would occur in the vicinity of the abrupt transitions, leading to the initiation and subsequent propagation of soil fracturing.

The traditional agricultural practice of Chinampas or “floating gardens” involved canals for irrigation and transportation purposes (see Fig. 23). As these agricultural lands are developed to accommodate the expansion of Mexico City, the infilled canal and adjacent floating gardens could create a physical setting involving abrupt transitions of different subsoils, depending on fill materials used as well as details of backfill construction.

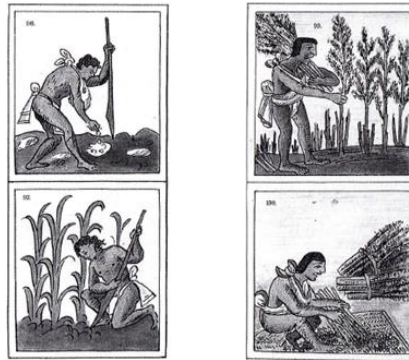


(a) Tree-lined canal

(b) Schematic illustration of “floating” garden



(c) Chinapass in plan view



(d) Schematic sketches of Chinapass practice

Fig. 23 Chinapass or “floating garden” agricultural practice in shallow lake (from Sabloff 1997)

Site 2: Colonia Del Mar Ground Cracking and Settlement, Tlahuac

Figure 24 shows a Google Earth map of the area of Colonia Del Mar, Tlahuac within La turba and Canal de Chalco (north-south main roads) and Langosta and Pirana (east-west main roads) the team visited on Oct. 17 (east of Camaron) and Oct. 18 (west of Camaron), where wide-spread ground cracking and settlement occurred. Figure 25 shows the location of the borough of Tlahuac in south Mexico City and some of the team’s observed ground cracks and settlements superimposed on the local street map. Also

shown in the figure is the location of the former Lake Texcoco, also illustrated in Fig. 13(c). More thorough mapping of these crack/settlement observations is given in a report from UNAM (Garcia 2017).



Fig. 24 March 2017 Satellite imagery of Colonia del Mar (Google Earth)

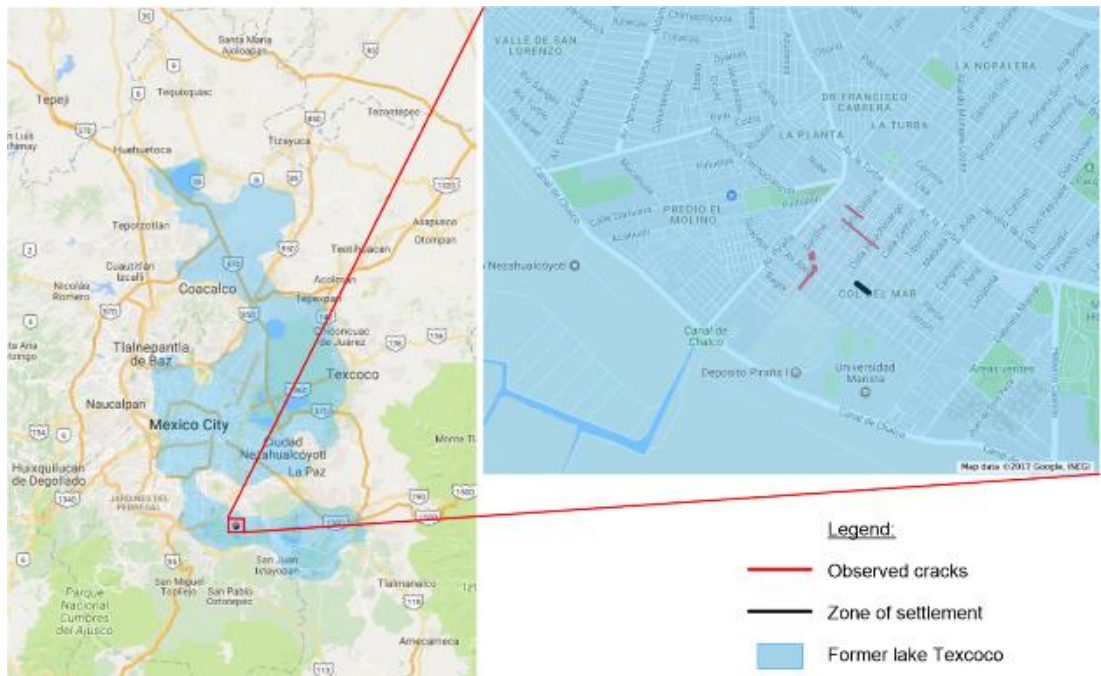


Fig. 25 Map of Tlahuac and location of the cracks observed by the CAEE team

Two features were observed by the GEER (2008) team in the area: (1) pipeline breaks; and (2) ground cracking and settlement. They appeared to be related to the phenomenon of soil fracturing as described by Auvinet et al. (II.UNAM 2017a). Historical satellite imageries on Google Earth show rapid development of the Colonia del Mar (Site 2) and Cienega San Gregorio (see Site 3 below) areas in recent decades. The observed pipeline breaks and ground cracking and settlement seem to reflect this sudden intensification of ongoing soil fracturing due to September 2017 seismic events. Figure 26 shows two scenes of settled

street involving both horizontal and vertical surface deformation. The alignments of settlements/cracks form some patterns on the scale of street-blocks. Buildings in the area showed varying degrees of distress as they accommodated the ongoing development of ground settlement and crack (see Fig. 27). The street level appears to have undergone significant change in front of the building with the Mexican flag. Pipeline and manhole repair and a street intersection are shown in Fig. 28.



Fig. 26 Ground settlements and cracks seemed to follow some patterns at street-block scale



Fig. 27 Buildings showing varying degrees of distress imposed by ongoing ground settlement and crack



Fig. 28 Pipeline and manhole repair (left) and street scene at an intersection (right)

Site 3: Ground Cracking, Xochimilco

Ground cracks were observed in Xochimilco (Site 3) at several locations, particularly in San Gregorio Atlapulco (see Site 4 below). Figure 29 shows the location of Xochimilco and San Gregorio Atlapulco. The areas are in agricultural districts with vegetable-flower fields and nurseries; where Chinapass or “floating garden” agricultural practice (see Fig. 23) was once used when a shallow lake was still present in the areas. Ground cracks show up in the vicinity of a surface drain inlet (Fig. 30), through an open field

(Fig. 31) and through a drive way (Fig. 32). These cracks seemed to be somehow related to the present or historical drainage features.

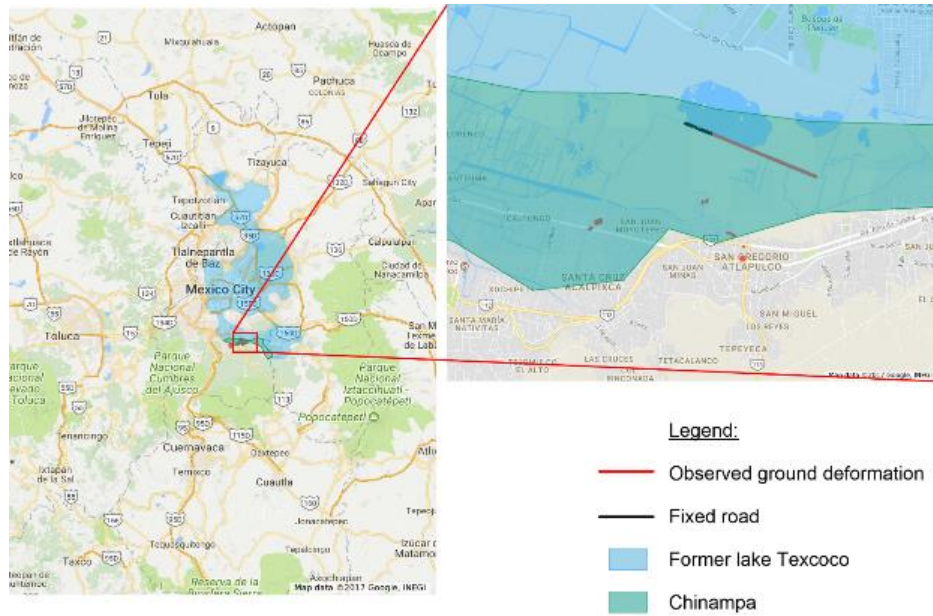


Fig. 29 Map of Xochimilco and location of the cracks observed by the CAEE team



Fig. 30 Cracks in vicinity of a surface drain inlet



Fig. 31 Cracks through an open field



Fig. 32 Cracks through a driveway

Site 4, Causeway Lateral-Spread, San Gregorio Atlapulco

Figure 33 shows a slumped causeway being repaired. The slumped segment underwent lateral spreading failure involving soft lake deposits beneath the granular embankment fill. The repair was carried out by bulldozers and dump trucks using granular fills borrowed from nearby quarries.



(a) Lateral spreading of causeway towards both sides (b) Repair by placing additional embankment fill

Fig. 33 Causeway embankment failure due to lateral spreading

Site 5: Repair of Slumped Masonry Canal Side Wall

A masonry side wall, covered with a wire mesh, performed well in general with the exception of a local slumped segment shown in Fig. 34. The repair of the slumped segment was in progress. It appeared that a cofferdam (using white sand bags shown both above and below the side wall in the right photo) was being built with a backhoe, probably for purposes of later dewatering during construction of the replacement masonry wall.



(a) End segment of slumped side wall (b) Repair of beginning segment of slumped side wall

Fig. 34 Repair of a slumped masonry canal side wall

## BUILDING DAMAGE

Building damage was primarily observed in non-ductile reinforced concrete frames with and without masonry infills, confined masonry buildings, as well as unreinforced load bearing masonry and adobe residential buildings. The building inventory consisted of pre-1985 poorly designed buildings and post 1985 well-designed buildings with seismic force resisting systems consisting of reinforced concrete frames or frame-shear wall interactive systems. It was observed that some of the post-1985 frame buildings were also damaged due to poor detailing. A great majority of buildings performed well.

The Mexico City seismic zones are discussed earlier and illustrated in Figs. 3 and 4. Unlike the interplate earthquake of 1985, which occurred off the coast along the Middle America Trench 350 km west of Mexico City and caused widespread damage to long-period structures in the central part of the city in two lake sub-zones with thicker soft clay deposits (Zone IIIc and III d), the intraplate earthquake of September 19, 2017 with closer proximity and different frequency content produced spectral peaks between 1.0 and 2.0 sec in the transition zone (Zone II) and two lake sub-zones with thinner soft clay deposits (Zone IIIa and IIIb), damaging mid-rise buildings. Comparison of building response spectra for the September 19, 2017 and September 19, 1985 events on firm and soft soils are illustrated in Fig. 35. As shown in the figure, thickness of soft soil layers and their dynamic properties (i.e. stiffness and damping) can have profound influence on the structural response of the buildings. The response will depend on the natural period of the structure and foundation soils as well as the type of earthquake and its epicentral distance.

Figure 36 illustrates the Uniform Hazard Spectra (UHS) that is included in the new seismic design code of Mexico City as optional hazard values. The spectra are expressed as a function of site period and can be used in conjunction with the site periods ( $T_s$ ) listed in Table 2. This table indicates that the site period in Zone III varies between 1.05 s for Zone IIIa and 2.26 s for Zone III d.

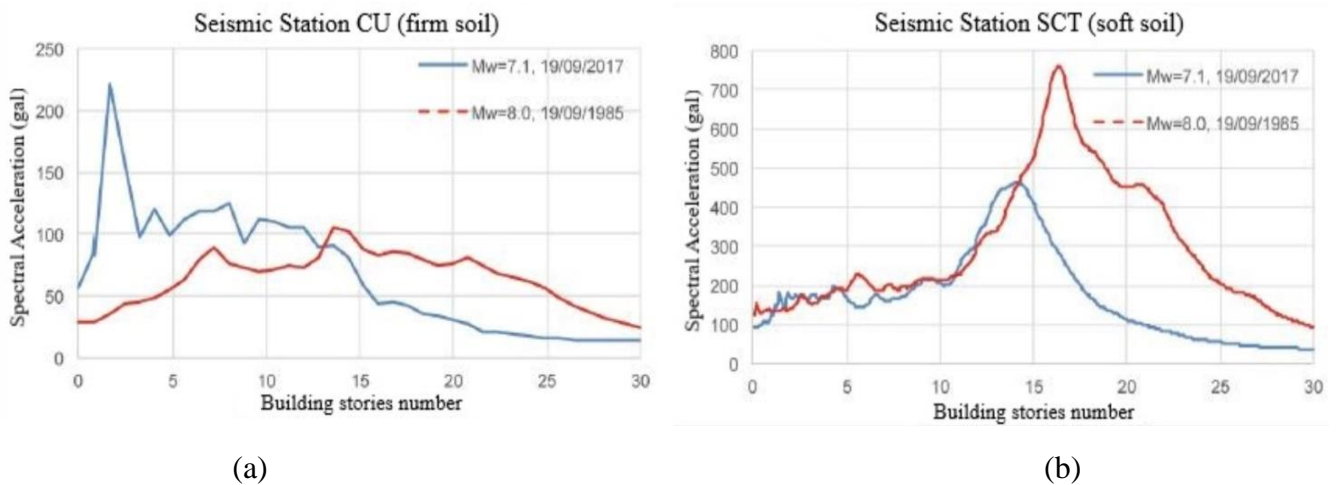


Fig. 35 Spectral accelerations experienced on roofs of buildings with different height, (a) at Station CU, located on firm soil or rock and (b) at Station SCT, located on lake zone

(Modified from Cruz et al. 2017)

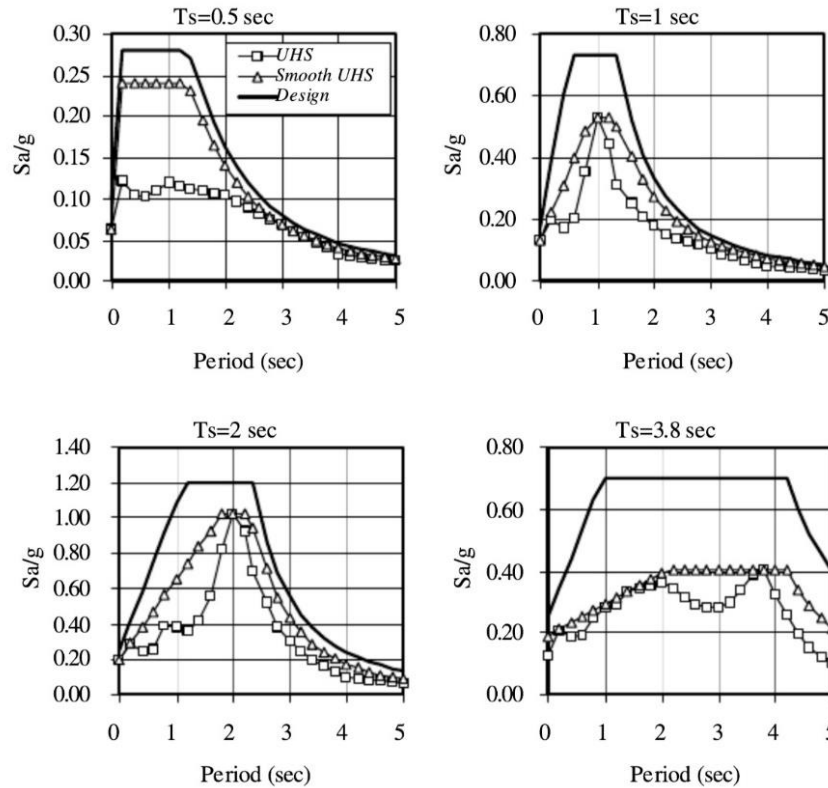


Fig. 36 UHS specified in the 2004 Mexico Building Code (Ordaz and Meli 2004)

Fig. 37 shows the design response spectra specified by the National Building Code of Canada (NBCC 2015) for Vancouver, Canada, the most populous city in Western Canada with similar seismicity as Mexico City. The shear wave velocity in different zones of Mexico City is listed in Table 2. Accordingly, the shear wave velocity ranges between 117.4 m/s and 81.8 m/s for Zones I and Zone III(d), which corresponds to Site Class E ( $V_s < 180$  m/s) based on the NBCC-2015 classification, indicating soft soil.

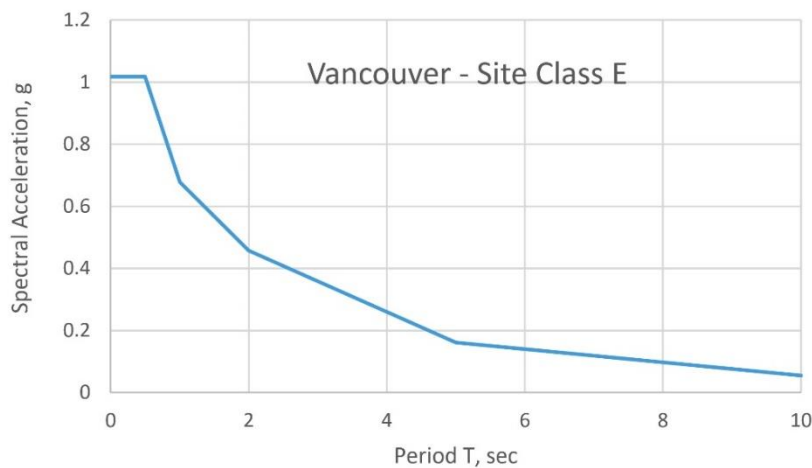


Fig. 37 Uniform Hazard Spectra for Vancouver, Site Class E (soft soil) as per NBCC-2015

Comparisons of design spectral values for Vancouver with those for the September 19, 2017 event presented in Fig. 7 indicates that buildings with approximately 1.0 s period in Vancouver could be vulnerable to similar ground shaking, if located on similarly soft soil without sufficient building ductility. The average peak ground acceleration (PGA) recorded in Seismic Zone III, Lake Zone, during the earthquake from records having an average epicentral distance of 115 km varies between 0.155g and 0.107g. In comparison, the NBCC-2015 lists the maximum PGA for use in design as 0.369g for Vancouver.

### Non-ductile reinforced concrete frame buildings

One of the common features of reinforced concrete frame buildings in Mexico, often with masonry infill walls, was lack of ductile detailing in reinforced concrete columns and the use of strong beams and weak columns. Figure 38 illustrates a 3-storey reinforced concrete frame building with exterior masonry infill walls. It was being used as a sports facility with open interior space. The building suffered from the hinging of columns, top and bottom, when the strong and rigid floor system used transferred seismic forces. The failure was in the form of the collapse of second and third floor columns. The building was designed and built in the pre-1985 era with poor seismic design practices. Another potential factor for the collapse was the rear support of the building, which consisted of a slender confined masonry wall with small size columns and confined brick masonry, as illustrated in Fig. 38(c).



Fig. 38 Lack of sufficient bracing and use of strong beams - weak columns

Lack of column transverse reinforcement was evident in older pre-1985 buildings. Figure 39 illustrates diagonal tension failure of one of the first storey columns of a multi-storey reinforced concrete frame building with masonry infill walls located in the Piedad Narvarte district of Mexico City. The figure also illustrates buckling of column longitudinal reinforcement near the previously opened wide diagonal cracks. Similar diagonal tension cracks were observed in other older residential construction. Figures 40(a) and (b) illustrate diagonal cracks in the first storey columns of a frame building with a soft storey. Figure 41(a) illustrates a rectangular column with diagonal shear cracks and Fig. 41(b) shows lack of concrete confinement due to insufficient transverse reinforcement in a residential building, hence resulting in the formation of a plastic hinge at the top. Lack of sufficient transverse column reinforcement could be seen in a number of different buildings as further illustrated in Fig. 42, which shows columns of an office building with insufficient buckling restraining ties and buckling of longitudinal bars in compression. All of these buildings were designed and built prior to the revisions of the seismic detailing requirements after the 1985 Mexico City Earthquake. However, one of the newer 5-storey reinforced concrete residential buildings, designed after 1985, also suffered column damage though the building in general performed well. One of the factors contributing to the column damage in this case was widely spaced column ties, as illustrated in Fig. 43, while the short column effect has also contributed to the increased seismic demand.



Fig. 39 Lack of sufficient column transverse reinforcement for diagonal tension

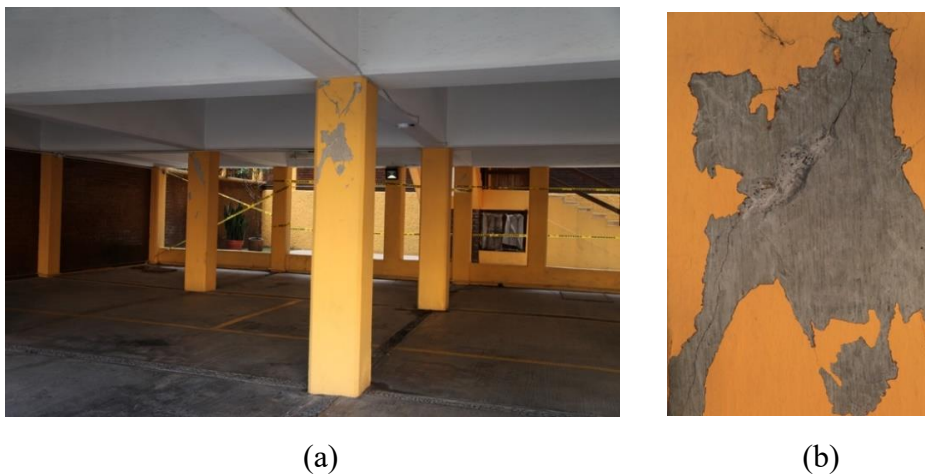


Fig. 40 Lack of transverse column reinforcement (a) diagonal tension cracking caused by increased shear demands in a soft-storey (b) close-up view



(a)



(b)

Fig. 41 (a) Shear cracks in a rectangular column of a soft-storey; the use of rectangular columns in the form of narrow shear walls saved the building, while the adjacent building suffered from complete collapse, (d) lack of concrete confinement and column hinging in an apartment building.



(a)



(b)

Fig. 42 Insufficient buckling restraining ties in a column and bar buckling

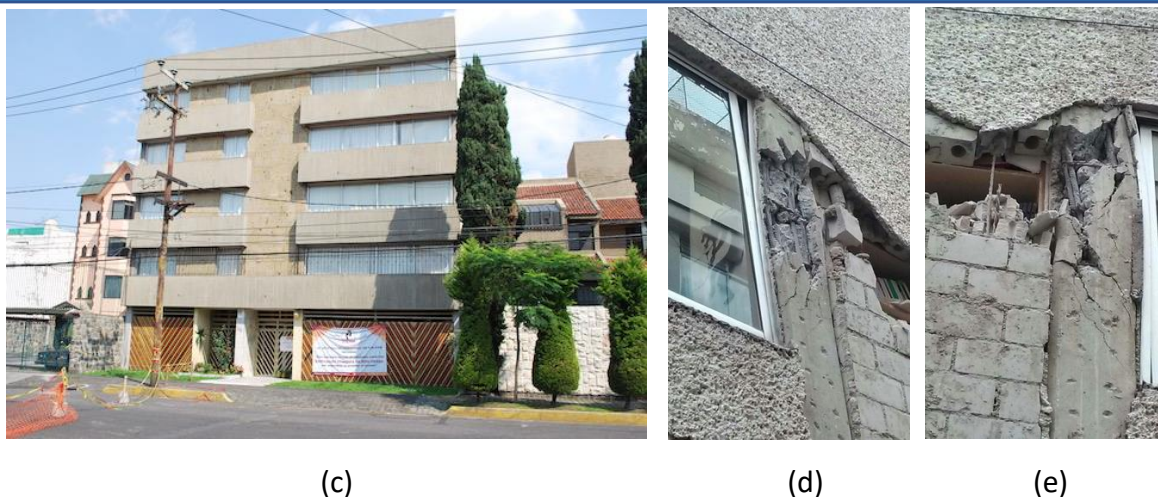


Fig. 43 Post-1985 reinforced concrete frame building with masonry infill walls and insufficient column transverse reinforcement

### Performance of retrofitted buildings

A number of reinforced concrete frame buildings were retrofitted after the 1985 Mexico City Earthquake. The retrofit techniques inspected during the reconnaissance visit included column strengthening and frame bracing. Two buildings were in the process of being retrofitted during the visit.

Figure 44 illustrates a typical column strengthening technique used in Mexico City. The figure illustrates retrofitting of Telmex Mexican Telecommunication Company building in Mexico City. The technique consists of steel angles placed longitudinally at each corner of a column, with steel strips welded to each angle in two transverse directions. The figure shows the application of the technique to a column that had already experienced some diagonal shear cracks during the September 19, 2017 Earthquake. It is interesting to note that the building had in-fill concrete panels in the short direction, as shown in Fig. 44(f), and the column shear cracks were associated with shear force reversals in the long direction. The same technique was used in an 8-storey reinforced concrete government building located near the San Antonio Abad subway station. The columns of the building were strengthened as shown in Fig. 45. However, this did not prevent the failure of columns and the collapse of the 4<sup>th</sup> floor in the corner, while many other columns in the building suffered varying degrees of damage. This retrofit technique was believed to have been used to increase shear reinforcement in the columns while also serving as buckling restraining ties. Indeed, the unretrofitted first-storey columns of the same building, shown in Fig. 42 indicate widely spaced small size perimeter and interior ties that were not able to prevent buckling of disproportionately larger longitudinal bars in compression. The same column retrofit technique was used for columns of a pre-1985 condominium in Calle Sonora Esquina Parque district, shown in Fig. 46, which suffered the collapse of a floor at the adjacent building roof level possibly due to the increased shear demands associated with pounding. The column retrofitting was not effective in preventing the collapse of the floor in the building.



Fig. 44 Telmex Telecommunication Company first storey column retrofit after the earthquake

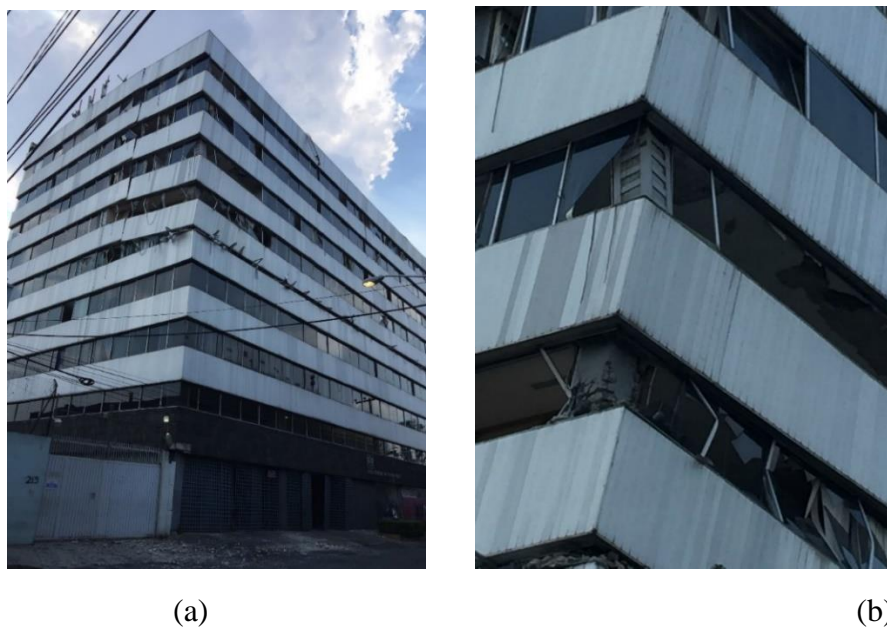


Fig. 45 Failure of the fourth floor of the office building near San Antonio Abad Subway Station in

Mexico City

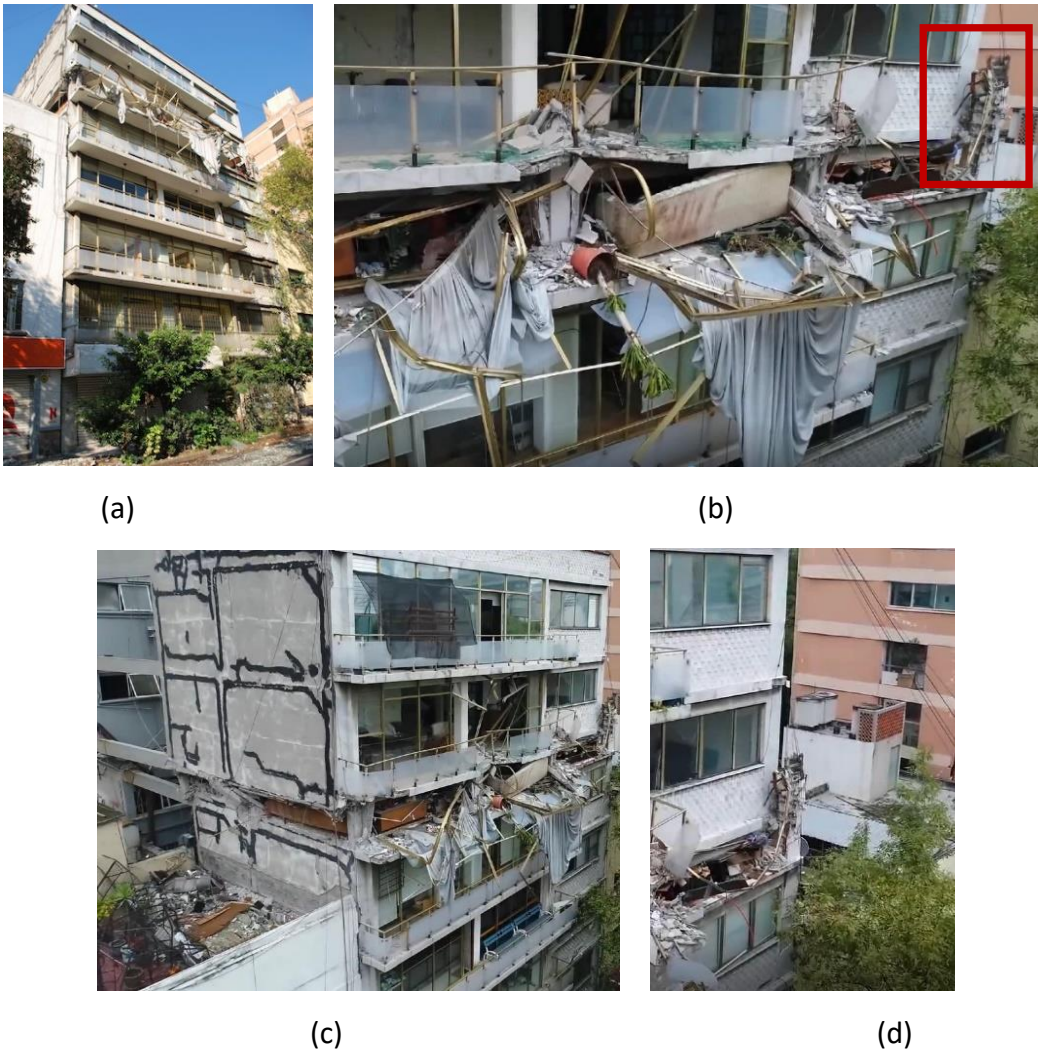


Fig. 46 Pre-1985 condominium in Calle Sonora Esquina Parque district with retrofitted columns that suffered the collapse of a floor at the adjacent building roof level possibly due to increased shear demand associated with pounding.

Another seismic retrofit method used in Mexico City was bracing of frame buildings with structural steel. Two of the buildings, one commercial and the other industrial, had been retrofitted with cross bracings prior to the earthquake and survived the ground shakings without any indication of damage. These buildings are shown in Figs. 47 and 48. Steel bracing of another reinforced concrete frame building that was under construction during the visit is illustrated in Fig. 49. It appears that, when seismic force and deformation demands are high, as in the case of soft stories or places of discontinuity, global interference such as the use of lateral bracing is a better choice than the retrofit of individual columns.

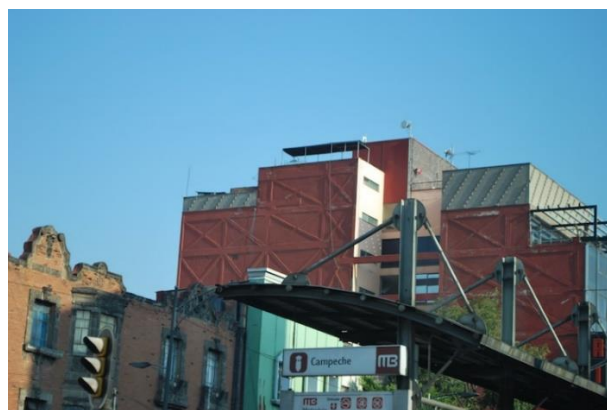


(a)

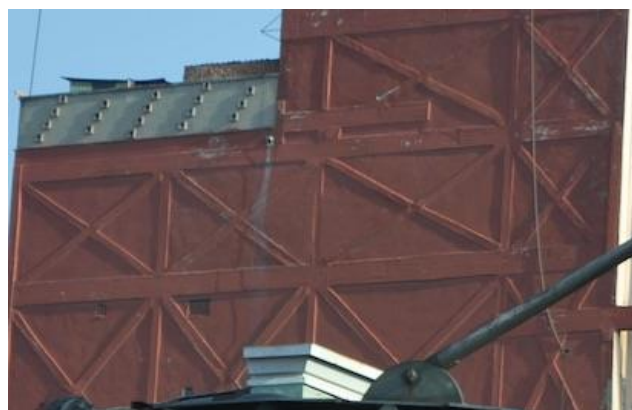


(b)

Fig. 47 Steel bracing of reinforced concrete commercial building



(a)



(b)

Fig. 48 Cross bracing of an industrial building



(a)



(b)

Fig. 49 Reinforced concrete office building being retrofitted after the earthquake with structural steel braces

## **Performance of masonry buildings**

Masonry structures in Mexico have been used since ancient times. Mesoamerican cultures built temples and housing complexes using mortared stone and adobe. In the colonial period, mortared stone masonry construction was often used for churches, castles, monasteries, aqueducts, and government buildings. Today, concrete block and brick masonry is widely used in low- and medium-rise construction in Mexico City due to its comparatively low cost and ease of use.

Historic buildings built using unreinforced, mortared stone lacked rigid diaphragms and details that would permit adequate transfer of forces at wall intersections and locations of plan discontinuities. Because of lack of proper connections and ability to transfer lateral forces, these structures are vulnerable to seismic excitations, experiencing considerable damage even under small magnitude earthquakes. Starting in the 1940s, masonry construction in Mexico relied on a system of confined, unreinforced, load bearing masonry panels surrounded by small cast-in-place concrete bond beams and tie-columns; the so-called confined masonry. Non-engineered confined masonry structures built before the 1985 Mexico City Earthquake had large spans between concrete columns with brittle details, such as the absence of tie-columns at wall intersections and bond-beams at wall ends – which made them vulnerable to strong earthquakes.

Mexico has a long tradition in the study and research about masonry, motivated by the large amounts of damage observed in unreinforced and non-engineered masonry structures during moderate to severe seismic events. After the Magnitude 8.1 - 1985 earthquake, the technical masonry standards of 1976 were reviewed with the objective of incorporating the knowledge acquired in Mexico as well as elsewhere in the World (Meli 1992). Because more than 70% of the buildings in Mexico are built with masonry, any improvement in design, construction and supervision of masonry projects is expected to have a significant economic impact.

### *Overview of Masonry Code*

The Mexico City Building Code (MCBC) is used not only in Mexico City but also as a model code in other states and municipalities. The MCBC comprises of a set of technical norms on different types of loading and on structural systems and materials with the masonry guidelines being referred as NTC-M (Alcocer et al. 2003). Allowable stress design was included in the first version of MCBC in 1942 while limit-state design was incorporated in 1976, including design material strengths and stiffnesses that were obtained from experimental research programs conducted in Mexico. After the 1985 Mexico City earthquake, the NTC-M was updated to incorporate the findings from the post-earthquake assessment. Although unreinforced and non-engineered masonry buildings fared poorly, well-constructed and well-designed masonry buildings were observed to have a satisfactory performance (Alcocer et al. 2003). This observation was again made during this reconnaissance visit, during which side-by-side comparisons between buildings of approximately the same size, basic floor plan, and age, showed that structures with good quality control and supervision during masonry construction had minimal damage. Because of the good performance observed for confined masonry structures, strength reduction factors were slightly increased in 1986 to counteract the increase in the design seismic shear coefficient adopted in the code. Confined masonry became widespread in Mexico in the 1940s as a method to control wall cracking due

to differential settlement that occurred on soft soil in Mexico City (Alcocer et al. 2003). Several years later, this system became popular in other areas of highest seismic hazard in Mexico due to its satisfactory earthquake performance (Meli and Alcocer, 2004). Confined masonry walls are confined vertically and horizontally with tie-columns and bond beams, respectively. These elements have small cross-sectional dimensions, typically equal to the wall thickness. Confining elements are intended to tie structural walls and floor/roof systems together, and improve wall energy dissipation and deformation capacities. Solid and hollow masonry units, either handmade or industrialized, are allowed for masonry construction.

The requirements of the current version of the masonry code for confined masonry at the time of the earthquake (NTC-M, 2004) are illustrated in Fig. 50. Accordingly, the distance between bond beams must not exceed 3 m while the spacing between tie-columns is the lesser of 4 m or 1.5 times the height of the building,  $H$ . Tie-columns must be placed at wall ends and wall intersections, and should be provided around openings whenever horizontal or vertical dimension of an opening are larger than  $\frac{1}{4}$  of the distance between the adjacent tie-columns or 600 mm.

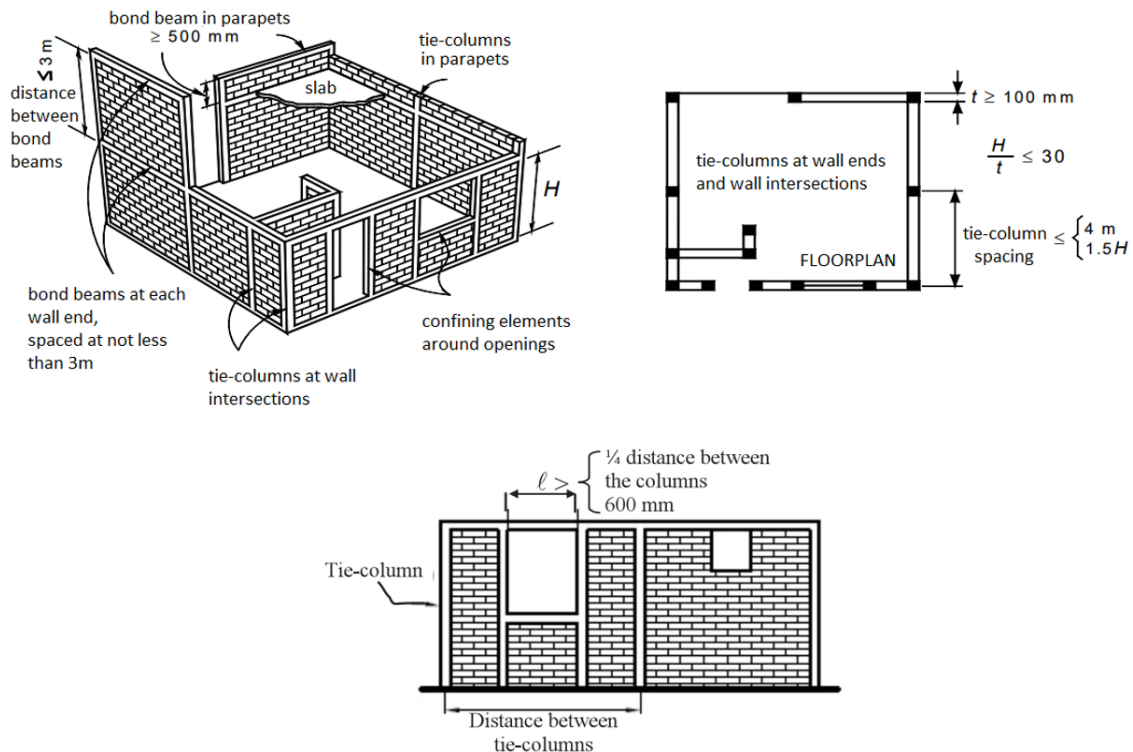


Fig. 50 Requirements for Confined Masonry. Adapted from NTC-M (2004)

In addition to confined masonry, partially grouted reinforced masonry wall systems are also used in Mexico (Fig. 51). Fully grouted, reinforced masonry is almost nonexistent. There is relatively low demand for this type of masonry and units that allow placement of internal reinforcement have to be requested by special order. Specified yield stresses of joint reinforcement typically vary between 500 to 600 MPa.

Unreinforced masonry is typically found in older construction and is discouraged by current code specifications. Reinforcement for structural integrity is required for this type of structures, placed vertically at wall intersections and at every 4 m, and horizontally along the top of the walls. The percentage of integrity reinforcement is approximately two thirds of that required for confined masonry structures. The seismic reduction factors in the Mexican norms are quite stringent (NTC-M, 2004). It is permitted to lower the seismic forces by a seismic performance factor of  $Q = 2.0$  if the confined masonry has solid units, and  $Q = 1.5$  if it has hollow units. Lateral displacement/drift limit of 0.25% is prescribed for confined masonry buildings with no horizontal reinforcement in the walls, and 0.35% when horizontal reinforcement is provided. These limits are substantially larger than the 0.15% drift limit prescribed for unreinforced masonry buildings.

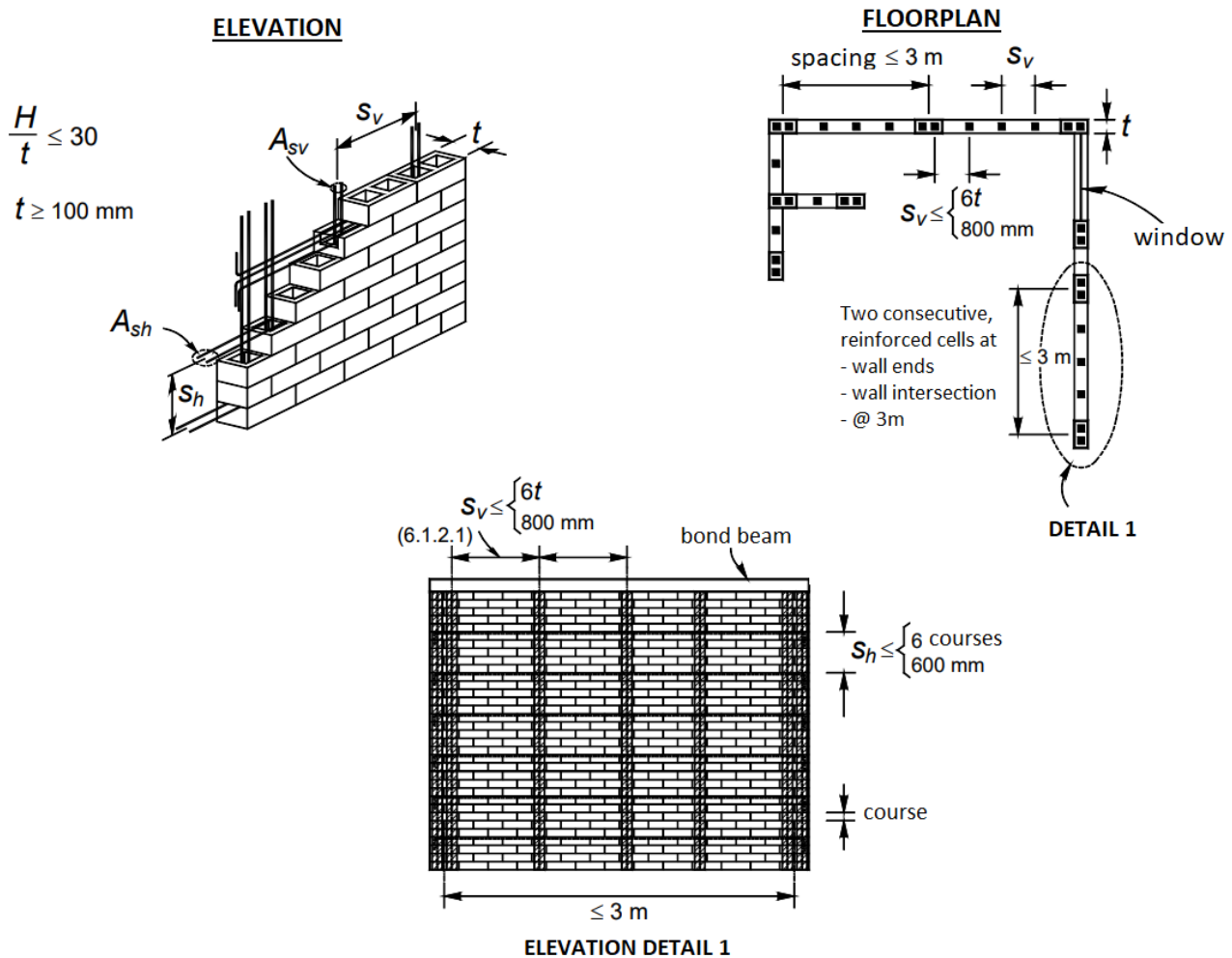


Fig. 51 Requirements for Reinforced Masonry (adapted from NTC-M 2004)

Confined masonry buildings

Some of the older confined masonry buildings constructed prior to 1985 suffered damage due to lack of proper detailing. A number of apartment buildings visited by the team in the borough of Tlalpan, south of Mexico City, showed poor detailing of load bearing walls, tie columns and bond beams. Figure 56(a)

shows three attached condominium buildings of similar structural configuration. Figs. 52(b) and (c) illustrate lack of sufficient column ties and Figs. 52(d) and (e) show lack of continuity of reinforcement between tie columns and bond beams. The interior and exterior masonry walls suffered significant damage in the form of diagonal shear cracks. This is illustrated in Fig. 53. However, reasonably good size columns and beams used around the perimeter of the buildings helped maintain the gravity load carrying capacity even after losing the load bearing masonry walls, as illustrated in Fig. 53(c) and (d).



Fig. 52 Pre-1985 confined masonry 5-storey residential building with poor detailing

Another example of poorly built confined masonry residential building is shown in Fig. 54. This building also belongs to the pre-1985 building inventory, and did not have tie columns around the openings. The use of longer spans between the tie columns, contrary to the requirement of the masonry code NTC-M, 2004, was also observed.

Combined use of reinforced concrete frames with confined masonry was observed in some older residential buildings. The 6-storey residential building shown in Fig 55 located in the Tlalpan district of Mexico City had the entire first floor that was built using rigid reinforced concrete frames with upper floors constructed using confined masonry, resulting in significant strength and stiffness discontinuity. As depicted in Fig. 55, the entire confined masonry segment above the first floor level suffered complete collapse. Another contributing factor to the building collapse was the alterations introduced to building configuration over the years. Originally, the building had an open first floor as shown in Fig. 55(a) when it was built in 1957. Subsequently, a large number of masonry partitions were added to create administration offices for the building, which increased the rigidity of the first storey compared to the rest

of the building as depicted in Fig. 55(b). Furthermore, there were 40 apartment units distributed over the upper five floors with a 6 m by 54 m floor plan. Some of these apartments were modified structurally without engineering input, as the owners removed interior load bearing walls in the weak direction to create more space. The weakened seismic resistance in the short direction, lack of expansion joints and insufficient shear walls in the short direction contributed to the failure.



Fig. 53 Damage to brick masonry walls in confined masonry buildings

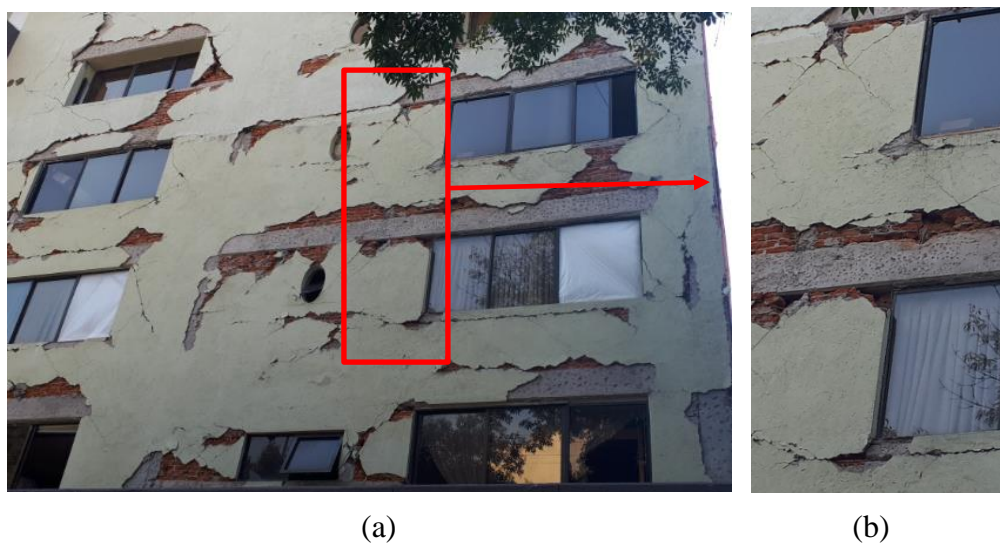


Fig. 54 Confined masonry building (Condesa, Cuautemoc, Mexico City).

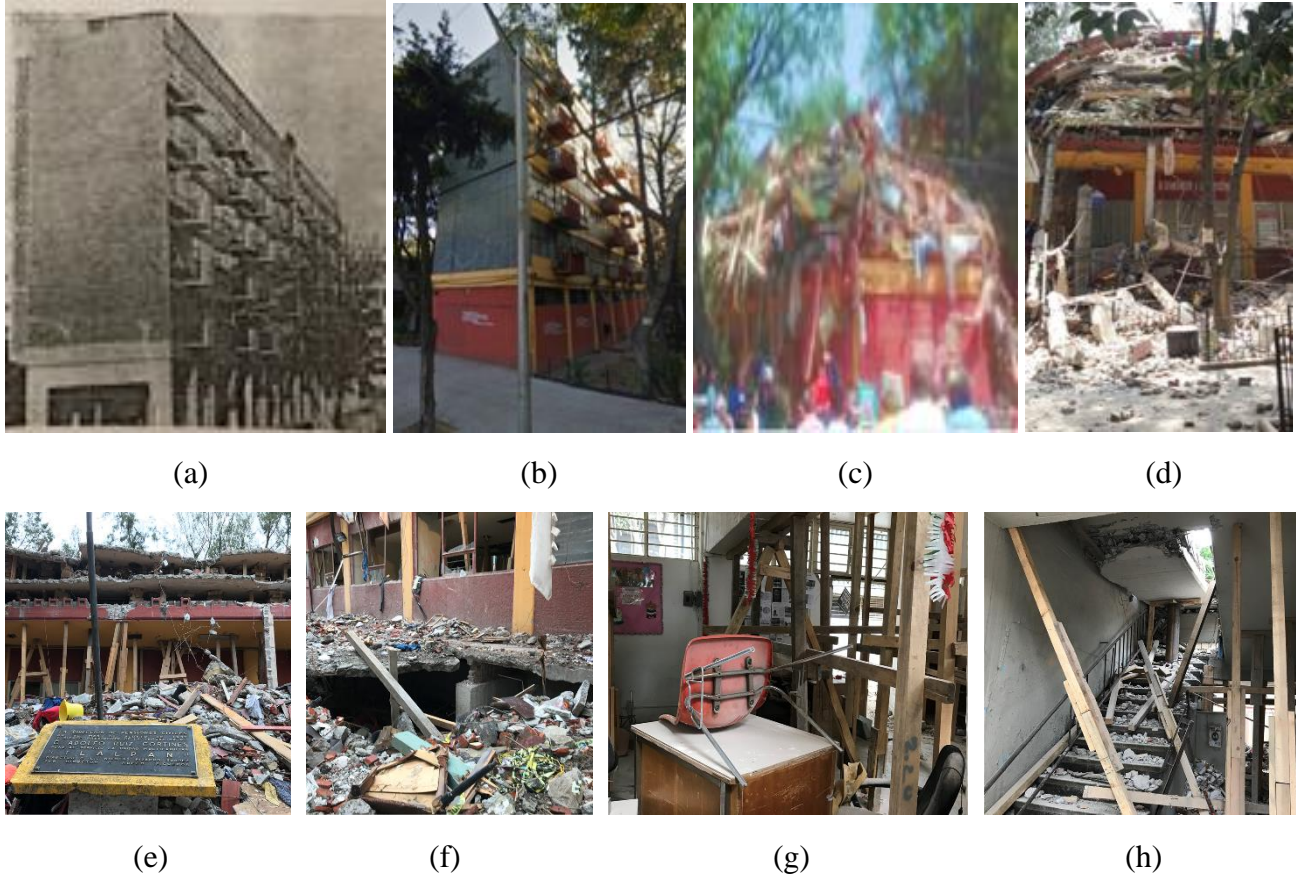


Fig. 55 6-Storey residential building in Tlalpan, Mexico City, (a) original configuration in 1957, (b) before the earthquake after the structural alterations, (c) few minutes after the collapse, (d) view of the longitudinal elevation after the earthquake.

Photos taken on October 17, 2017 are shown in Figs. 55(e) to 55 (h): pancaked 2<sup>nd</sup> and 3<sup>rd</sup> floors over the intact first floor at the back of a building plaque, Fig. 55(e); an opening to the foundation floor beneath the first floor visible in Fig. 59(f); interior of a room on the first floor, Fig. 55(g); and a staircase on the same floor, Fig. 55(h). Both the interior and exterior conditions of the first floor were remarkably good, after sustaining the impact of the fallen upper floors. The unfortunate irony was the fact that the intact floor was the only unoccupied floor in the entire building at the time of earthquake.

Although the majority of damaged confined masonry buildings were representative of older practice, a few buildings designed and built after 1985 also suffered damage. Figure 56 shows a confined masonry apartment building on Zapata Street in the Coyoacan district of Mexico City that was built in 2016. The building suffered partial collapse, which was attributed to widely spaced tie columns and poor performance of columns due to the buckling of longitudinal reinforcement. The column transverse reinforcement had a 250 mm spacing, which violated the masonry code NTC-M (2004) requirement of the lesser of 200 mm or 1.5 time the least column dimension. Figure 60 shows the building after the earthquake.

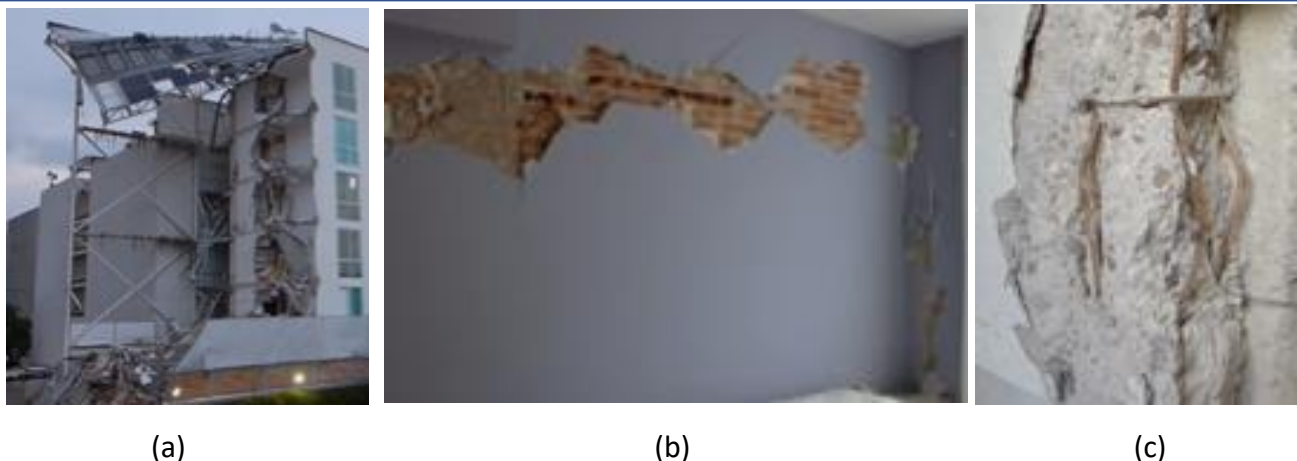


Fig. 56 Confined masonry apartment building built in 2016 (Zapata St., Coyoacan, Mexico City, (a) partial collapse of the building, (b) wide spacing of tie columns, (c) wide spacing of column ties and buckling of longitudinal reinforcement.

#### Partially reinforced masonry buildings

The majority of load bearing masonry buildings consisted of unreinforced masonry (URM) construction. Very few partially reinforced and partially grouted masonry buildings were used in Mexico. Figure 57 illustrates a partially reinforced and partially grouted masonry building in Cuauhtemoc, Mexico City. The figure shows typical damage observed in the form of wide diagonal and horizontal cracks. Figures 57(b) and (d) show lack of tie-columns over a large span (approximately 8.0 m). Furthermore, the code for masonry (NTC-M, 2004) specifies that at least two consecutive reinforced cells should be used in wall intersections and at wall ends in addition to those required by structural analysis. This requirement was not complied with in this building. Also, no horizontal reinforcement was observed in the infill walls, contrary to the code recommendation of placing horizontal reinforcement at least every 6 courses or every 600 mm, whichever is less.

#### Damage to non-structural masonry infill walls

The use of masonry as in-fill walls either as part of the building envelop or for interior separation of space is common in Mexico. These wall are intended to fulfill their non-structural functions, often participate in lateral load resistance due to improper isolation from the enclosing structural framing elements. In buildings with high wall to floor area ratios and in the absence of structural shear walls, they did help maintain structural integrity, but developed excessive cracking an partial collapse. Figure 58 illustrates damaged infill walls due to diagonal tension cracking associated with shear forces transferred from the attached structural elements.



Fig. 57 Partially reinforced and partially grouted masonry building (Cuauhtemoc, Mexico City)



Fig. 58 Diagonal tension cracks in infill brick masonry walls of two reinforced concrete frame buildings in Cuauhtemoc, Mexico City, (a) wall in a post-1985 building, (b) wall in a pre-1985 building.

Some of the perimeter walls also suffered from out-of-plane failures. Figure 59 shows an industrial building that developed out-of-plane failures of slender concrete block masonry walls. These walls were confined with tie columns and bond beams.



Fig. 59 Out of plane failure of concrete block masonry walls

#### Traditional non-engineered masonry and adobe buildings

Traditional non-engineered masonry and adobe construction is very common in rural area of Mexico. Simple form of confined masonry, built by local tradesmen or homeowners, without adhering to any code or standard resulted in massive destruction of buildings. Figure 60 illustrates examples of such destruction in the state of Morelos. The figure also demonstrates the type of construction practices employed, mostly consisting of brick load masonry walls, with or without small size concrete tie columns of low quality concrete, and sometimes locally found stones replacing bricks. These buildings are often limited to two stories, with wood roofs sometimes carrying heavy roofing tiles.

Adobe houses are built using thick, handmade units. This type of construction is extremely brittle and often suffers from complete collapse when subjected to strong ground excitations. Figures 61 shows examples of destruction of adobe houses in the state of Morelos. Figures 61 and 62 show similar destruction in rural Xochimilco, just south of Mexico City. Adobe houses are built with lighter wood roof. However, sometimes owners interfere with the construction and make alterations that have structural implications. The original wood roof of the adobe house shown in Figs. 62(c) and (d) was replaced by a thick concrete roof, which attracted high seismic forces, resulting in the total destruction of the house.

#### **Buildings with soft stories**

The use of open space at the first-storey level of residential buildings is common in Mexico City. This space is often used for parking, creating soft stories and associated vertical stiffness and strength irregularities. Soft stories usually have reinforced concrete frames, often with small size columns having limited shear capacities, as well as limited inelastic deformability. Upper floors either have load bearing masonry walls or reinforced concrete frames with masonry infills. The use of soft stories was forbidden in the 2004 Mexico City Seismic Code (NTC-DS 2004).



Fig. 60 Collapse of non-engineered buildings in the State of Morelos



Fig. 61 Adobe construction in the State of Morelos

Figure 63 shows a reinforced concrete frame with a soft storey and masonry infill walls above the first floor. The columns of the building suffered shear damage and developed extensive diagonal tension cracking as illustrated earlier in Figs. 63(a) and (b). Another example of a soft-storey reinforced concrete building damage is illustrated in Fig. 64 where two residential buildings were located side by side, one with reasonably sized rectangular columns that survived the earthquake with diagonal tension cracking in the columns, but the nearby building collapsed, losing the first storey parking area. Other examples of soft storey performance, often resulting in the failure of reinforced concrete columns with insufficient strength and deformability leading to the collapse of the entire first-floor, are illustrated in Figs. 65 and 66.



(a)



(b)



(c)



(d)



(e)



(f)



(g)

Fig. 62 Failures of adobe buildings in Xochimilco, Mexico City



(a)



(b)

Fig. 63 Reinforced concrete frame building with a soft storey in Mexico City.



(a)



(b)

Fig. 64 Failure of a soft storey in a reinforced concrete frame residential building.



(a)



(b)

Fig. 65 (a) Collapse of a soft storey over reinforced concrete columns, (b) crushing of a first-storey column



(a)



(b)



(c)



(d)

Fig. 66 Soft storey failures (a) Balsas St, Benito Juarez, Mexico City, (b) Saratoga St, Benito Juarez, Mexico City, (c) Tokio St, Benito Juarez, Mexico City, (d) Coquimbo St, Gustavo A. Madero, Mexico City

Figure 67 shows the 8-storey reinforced concrete frame residential building with brick masonry infill walls at the intersection of Enrique Rebsamen and La Morena Streets in Mexico City. The building had a soft storey, which increased seismic shear demands on the first storey columns, which had not been designed using seismic detailing. The columns suffered significant damage and the core concrete crushed in a number of columns as illustrated in Fig. 67. The column ties were 150 mm apart, having 90-degree bents. The longitudinal reinforcement buckled and many columns lost their gravity load carrying capacities. Other examples of soft storey performance, often resulting in the failure of reinforced concrete columns with insufficient strength and deformability and the collapse of the entire first floor, are illustrated in Figs. 68 and 69. The building on Enrique Rabasamen street (No: 241), only two building away from the building shown in Fig. 67, lost its first floor completely (see Fig. 68). The building could collapse if it did not lean against the nearby building. Figure 68(b) illustrates the demolition of the building after the earthquake. Similar behaviour was observed in other older reinforced concrete frame buildings with soft storeys, as shown in Figs. 69 (a) and (b). However, a nearby residential building, though had a soft storey, remained intact because of the shear walls provided at the first-storey level. This is illustrated in Fig. 69 (c).

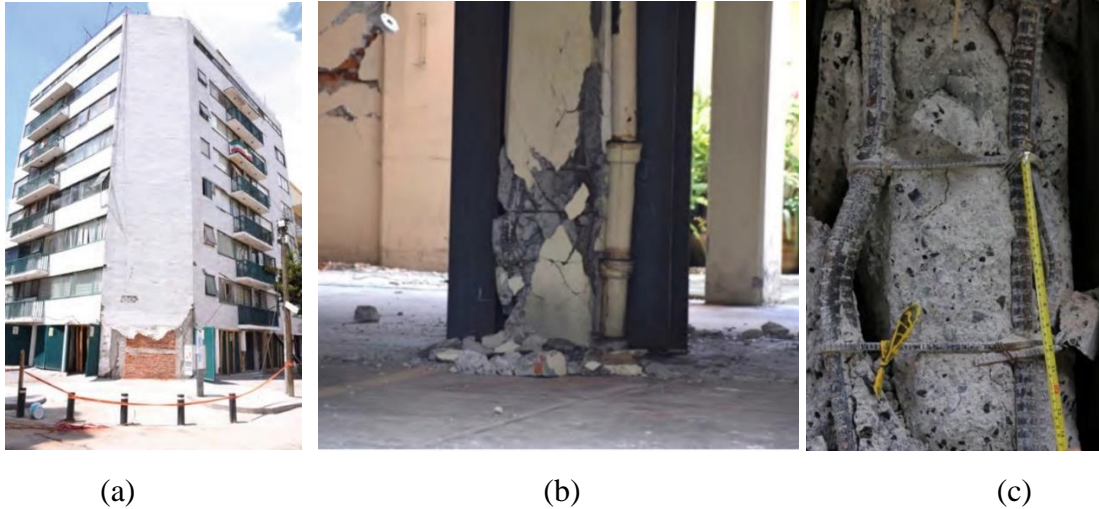


Fig. 67 Soft storey of a reinforced concrete frame building at 249 Enrique Rebsamen Street



Fig. 68 Soft storey failure of a 5-storey reinforced concrete residential frame building at Enrique Rabasamen street (No: 241), (a) after the earthquake, and (b) during demolition

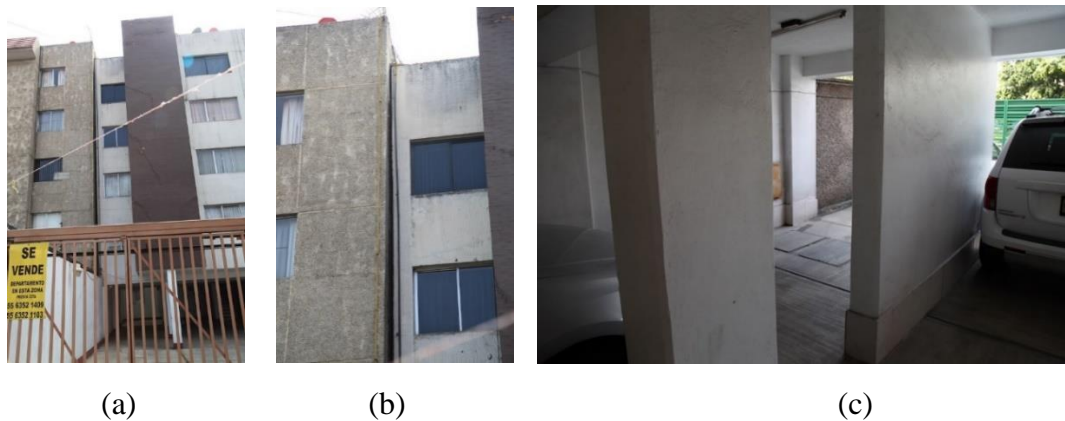


Fig. 69 (a) and (b) 5-storey residential building with reinforced concrete frames and a soft storey, leaning against the adjacent building, (c) a nearby reinforced concrete residential building first storey concrete shear walls preventing damage to soft storey

Figure 70 illustrates another example of soft storey damage to an older reinforced concrete frame building with poor column detailing. This building lost a number of columns due to lack of seismic detailing of transverse reinforcement as illustrated in the figure.



Fig. 70 (a) Building with a soft storey, leaning against the adjacent building, (b), (c), (d) damage to first-storey columns.

### **Pounding, separation, tilting and settlement of buildings**

The presence of lacustrine deposits in the Valley of Mexico basin resulted in foundation related structural problems. These include ground subsidence and settlement prior to the earthquake. A number of apartment buildings in the Cuauhtemoc Borough of Mexico City was observed to have pre-existing settlement and tilting of multistorey residential buildings. The reconnaissance team had difficulty judging whether the observed settlement and/or tilting of multi-storey buildings could be attributed to the earthquake or it existed prior to the seismic event. UNAM report (2017) provides a comprehensive background of this unique issue of soil subsidence and its effects on buildings over the years, covering its development over a period of six decades between 1959 and 2016. Figure 71 illustrates the uneven separation of two multistorey buildings in La Condesa, Mexico City. The building on the left was estimated to have rotated about 1 degree prior to the earthquake (GEER Report 2017).

According to the Mexican seismic guidelines (NTC-DS, 2004), the space between buildings should be greater than 50 mm plus the minimum lateral drift ratio defined for each zone. The minimum lateral drift ratios are defined as 0.1%, 0.3% and 0.5% of the building height for seismic Zones I, II and III, respectively. The minimum separation is to be calculated for each building on either side of the separation relative to the land boundary. This implies that the separation between two 8-storey buildings should be more than approximately 250 mm in Zone III. The observed buildings by the reconnaissance team did not have this level of separation and violated the current building code. Figure 72 shows typical building separation observed.



(a)

(b)

Fig. 71 11-Storey La Condesa building (on the left) that had tilted and rotated about 1 degree prior to the earthquake, (a) Google Street View photo of 2016, (b) building after the earthquake

(GEER Report 2017)



(a)



(b)

Fig. 72 Typical separation between buildings, less than that recommended by the Mexico City Seismic Code, (a) post 1985 building in Puebla, (b) pre-1985 buildings in Mexico City.

The lack of sufficient building separation, discussed above, led to the ponding of buildings, damaging many during the earthquake. Some buildings suffered damage along the separation, others suffered local damage at the location of discontinuity of one of the buildings, and some suffered complete failure due to the pounding of the adjacent building. The 8-storey reinforced concrete frame condominium building built in the pre-1985 era in Calle Sonora Esquina Parque district of Mexico City suffered complete collapse of the 6<sup>th</sup> floor, pounding on the nearby building, which was shorter. The failure of the 6<sup>th</sup> storey columns were discussed earlier in Fig. 46. A similar mid-height collapse of a complete floor occurred in the building immediately behind the building in Fig. 46. The failure was triggered by pounding against the shorter adjacent building. Figure 73 depicts the failure mode of the building. When buildings were of similar height and especially when the floor elevations lined-up, the damage due to the pounding effect was limited to local elements, as indicated in Fig. 74.



Fig. 73 8-Storey reinforced concrete building, with a collapsed intermediate floor due to pounding on the adjacent building (GEER Report 2017).

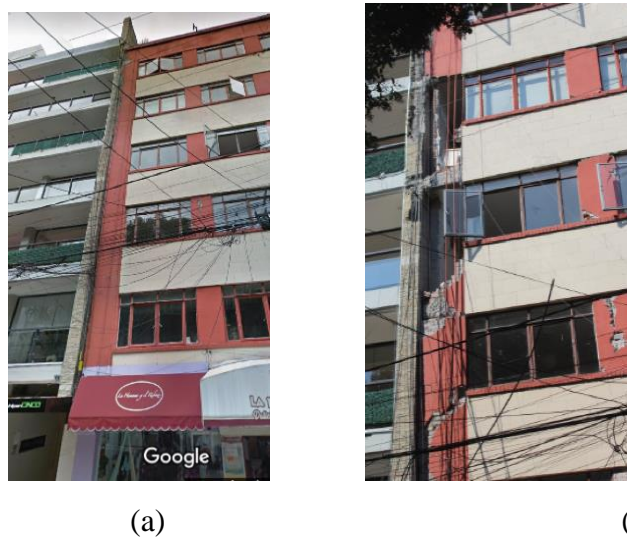


Fig. 74 Pounding of buildings (Chilpancingo St, Cuauhtemoc, Mexico City), (a) before the earthquake, separation not complying with the seismic code, b) local damage after the earthquake.

The reconnaissance team also observed many buildings that suffered from vertical settlement. The soft soil conditions of the region resulted in ground failures, as discussed earlier, also causing settlement of multi-storey buildings, without much structural damage. An example of vertical settlement can be seen in Fig. 75.



Fig. 75 8-Storey building on La Morena (716), foundation edge plunging into the ground (GEER 2017).

### Performance of newer buildings

The building design practices in Mexico City improved significantly after the 1985 Mexico City Earthquake as indicated earlier. The most recent edition of the seismic code is dated 2008 and reflects the improvements introduced after the 1985 event. Revised and improved edition of the code was expected to be printed in 2018. Buildings designed after the 1985 improvements performed well, except for some minor damage, essentially resulting from lack of proper implementation of seismic detailing practices. In newer buildings, the majority of damage was limited to damage to masonry infill walls, which often developed diagonal shear cracking. However, the lateral load resisting systems performed well in the post-1985 engineered buildings. Figure 76 illustrates two buildings in the Esquina Parque district, where older buildings suffered damage. These building performed well, with damage limited to the cracking of non-structural infill walls.



Fig. 76 Post-1985 buildings in Mexico City, showing superior performance

In the city of Puebla, in spite of the widespread damage observed in older reinforced concrete, confined masonry and more conventional masonry/adobe buildings, newly designed buildings after 2000 survived the earthquake with little damage, mostly to non-structural elements and exterior cladding. Figure 77 shows modern high-rise buildings at the north entrance to the city with no apparent structural damage. It is noteworthy that these buildings were taller than the older buildings, thus having longer periods.

Additional new buildings were inspected in the city of Puebla, mostly reinforced concrete, having lateral load resisting systems consisting of either shear walls or frames with infill walls. Figure 78 shows buildings with damage limited to masonry cracking, which was being repaired during the visit.

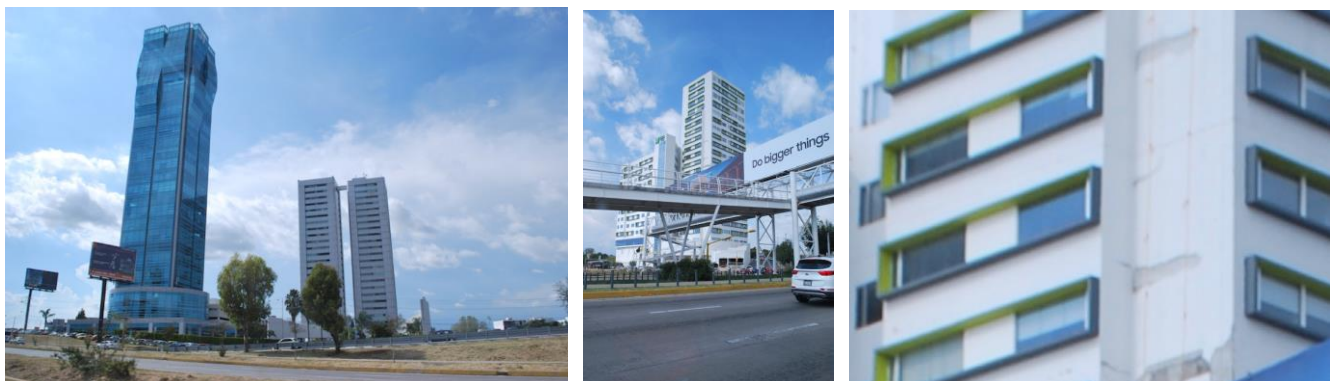


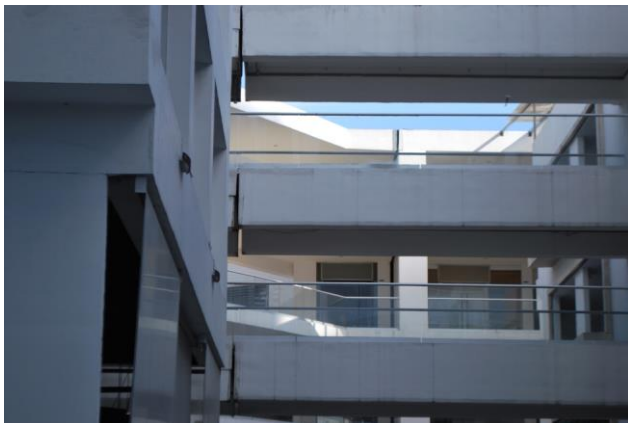
Fig. 77 Modern construction of post-2000 era in Puebla, (a) high-rise building with curtain wall cladding, (b) Holiday Inn buildings, reinforced concrete with masonry infill walls, (c) damage to the exterior cladding of the Holiday Inn building.



(a)



(b)



(c)



(d)

Fig. 78 Post 2000 buildings in Puebla, (a) and (b) residential multistory buildings, (c) and (d) separation of the bridge connecting parking structure to the nearby shopping centre.

### PERFORMANCE OF BRIDGES

Bridges are critical components in the transportation networks of large metropolitan cities, especially in Mexico City, which is the social, economical and national capital of Mexico. According to Yashinsky (2018), most of Mexico's bridges were designed and constructed before 1970, without consideration of seismic design. More recent and new bridge designs have adopted the American Association of State Highway and Transportation Officials (AASHTO) Bridge Design Specifications, which include seismic design requirements. Despite the majority of the bridges lacking seismic design, bridges generally performed well during the September 19, 2017 earthquake. Members of the reconnaissance team were able to visit four damaged bridge sites within the Mexico City areas to gather information, as well as bridge performance observation data on lessons learned from the Mexico earthquake experiences. The types of bridge damage observed include plastic hinge formation at a bridge pier column, foundation rocking, torsional movement of bridge girder, damage to shear key, large movement or deformation of

bridge bearings, longitudinal movement of bridge girders and abutment failure. These observations are described in the following sections based on the sites that were visited.

## Metro Line Viaduct

### Site 1

The Mexico City Metro system is the second largest mass transit network in north America after New York City. Metro Line 12 is the newest line in the Mexico City Metro system. It was opened in 2012. The elevated viaduct of Metro Line 12, shown in Fig. 79, consists of two steel girders at each span, simply supported on single 2.0m diameter circular reinforced concrete column bents with heavy cap beams. The steel girders support a concrete deck of width sufficient to accommodate two parallel tracks for trains running in opposite directions.



Fig. 79 Mexico Metro Line viaduct

The 2.0m diameter column of a span at the intersection of Av. Tlahuac and Calle Gitana between the metro stations Alvois and Nopalera of Line 12 was severely damaged with a plastic hinge forming at the base, as illustrated in Fig. 80(a). It was observed from the exposed rebars at the plastic hinge of the damaged column that there was very little or no transverse reinforcement of the column except for the top of the exposed plastic hinge region where some loose smooth tie bars could be seen. It was also observed that there was coupling of longitudinal reinforcement at the plastic hinge location, which could have adversely affected the ductility capacity of the column pier. Although the core concrete showed signs of beginning to crush, the longitudinal reinforcement seemed to remain largely intact without any sign of buckling or yielding. The level of damage could have been significantly worse if the strong ground motion of the earthquake was just a little longer. Upon further examination of the condition of adjacent columns, there was clear sign of rocking of the column piers during the earthquake as evident by the gap at the base of the adjacent columns after the earthquake. This is illustrated in Figure 81. It can be argued that this rocking motion may have reduced the seismic forces on the structure and prevented damage to the adjacent

columns. It is also possible that the rocking motion of the damaged column prevented it from suffering even more severe damage, such as buckling of the longitudinal rebars, leading to opening and further deterioration of the column at the plastic hinge region.



Fig. 80 (a) Damaged viaduct column (courtesy of C. Cruz-Noguez), (b) column after repair



Fig. 81 Sign of rocking movement of viaduct column

Figure 82 shows the response spectral acceleration of the ground motion from the September 19, 2017 earthquake recorded nearby, in Tlahuac, which is one of the 16 municipal districts of Mexico City. The stronger NE component of the recorded motion at the likely period of 1.0 s of the viaduct corroborates with the perpendicular direction of the viaduct. This correlates with the observed plane of vibration of the viaduct motion resulting in the orientation of the plastic hinge formed as depicted in Fig. 80(a).

After the earthquake, an emergency frame was erected around the damaged column to provide shoring support to the steel girders of the two adjacent viaduct spans, as illustrated in Fig. 83(a). The repair measure was concrete jacketing with steel forms, as shown in Fig. 83(b). The repaired column is also shown in Fig. 80(b). According to the Metro engineering personnel at the site, the column foundation was also repaired with new concrete, which can also be seen in Fig. 83(b). No further details could be obtained by the reconnaissance team.

### Tláhuac

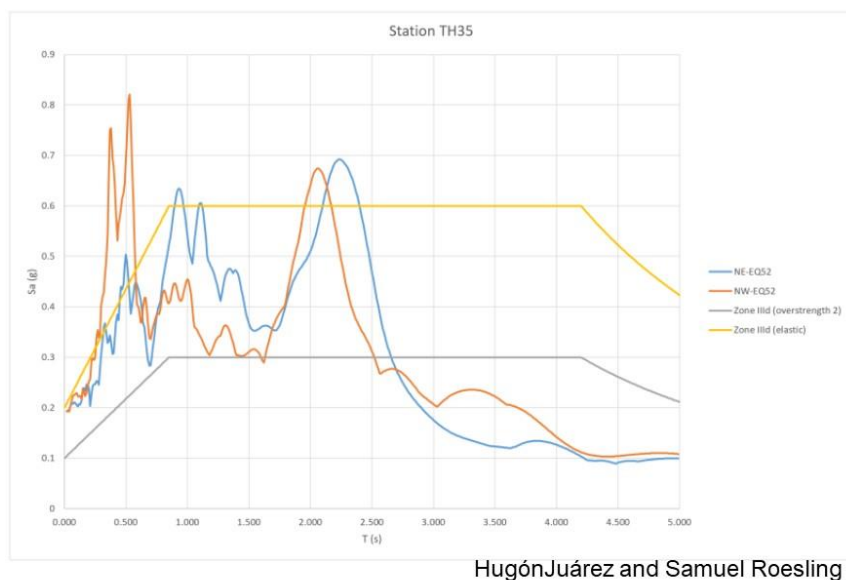


Fig. 82 Response spectral acceleration at Tlahuac, Mexico City, Mexico (HugónJuárez and Samuel Roesling)



(a)



(b)

Fig. 83 (a) Emergency support of damaged column (b) Repair of damaged column by jacketing

Site 2

At a distance 1.2 km south-east of Site 1, at the intersection of Av. Tlahuac and Av. Guillermo Prieto, the Metro Line 12 viaduct has the alignment layout of an S-shaped double curve, as shown in Fig. 84. At this location, damage was observed at the shear keys of a span with three steel girders. This was attributed to excessive movement of the girders in the longitudinal direction, resulting in complete spalling of the concrete restraint at the shear keys. This is illustrated in Fig. 85. Significant rocking of the column piers, possibly exacerbated by torsional response of the curved viaduct, was observed. Figure 86 shows cracks on the roadway next to a column pier at this location as evidence of the significant rocking response of the column pier during the earthquake. Torsional response of the curved viaduct could have further exacerbated the rocking of the piers. Figure 87 shows significant shift of the girders along the longitudinal direction of the viaduct. It was fortunate that the cap beam provided sufficient seat support length for the girders and prevented the collapse of the entire span of the viaduct. Figures 88 and 89 show significant shear deformation of bridge elastomeric bearings supporting the steel girders of the viaduct.



(a)

(b)

Fig. 84 Double curved Metro Line viaduct, (a) towards NW direction, (b) towards SE direction



Fig. 85 Failure of concrete restraint at shear key of viaduct



Fig. 86 Cracks on roadway due to rocking of viaduct pier



Fig. 87 Shift of viaduct girder



(a)



(b)

Fig. 88 Shear deformation of girder bearings



Fig. 89 Longitudinal displacement at deck level and lateral displacement

### Highway Overpass

The third bridge damage site visited by the reconnaissance team was a highway bridge located at Circuito Interior Avenida Rio Churubuscophotos in Mexico City. The bridge structure is shown in Fig. 90. It consists of two parallel underpass bridges. The 5-span bridge has wall piers and unreinforced masonry (URM) abutments. The URM abutments were damaged during the earthquake as shown in Fig. 91. Some reinforcement was observed at the exposed upper part of the abutment; but the lower main part of the masonry abutment was unreinforced. Figure 92 shows cracks and settlement in the surrounding ground due to significant rocking of the wall piers. Permanent tilting of some of the wall piers was clearly evident after the earthquake. This is shown in Fig. 93.

### Periferico South Pedestrian Overpass

When pedestrian overpasses are damaged, they can be closed to traffic with little impact on the transportation system. Similarly, if they collapse over a major route they are relatively easy to be removed, generally having high priority. This creates challenges for reconnaissance team members to identify the cause of the collapse if the visit is conducted afterwards. The fourth bridge, Periferico Pedestrian overpass near the intersection with Muyuguarda Street is an example. This overpass crossed a 4-lane divided highway, Periferico Ave (Adolfo Ruiz Cortines Blvd), with frontage roads. While the piers fared well, the south span of the superstructure appears to have displaced off the centre pier in the boulevard as illustrated in Fig. 94. In doing so, it collapsed on a taxi whose driver was fortunately able to escape through a window. No information on other injuries has been noted. The remaining spans were removed, as well as the collapsed portion of the bridge, prior to reconstruction.



Fig. 90 Parallel 5-span underpasses



Fig. 91 Damaged URM abutment



(a)



(b)

Fig. 92 (a) Rocking of wall pier, (b) crack and settlement of surrounding ground adjacent to wall pier



Fig. 93 Tilting of wall pier after earthquake

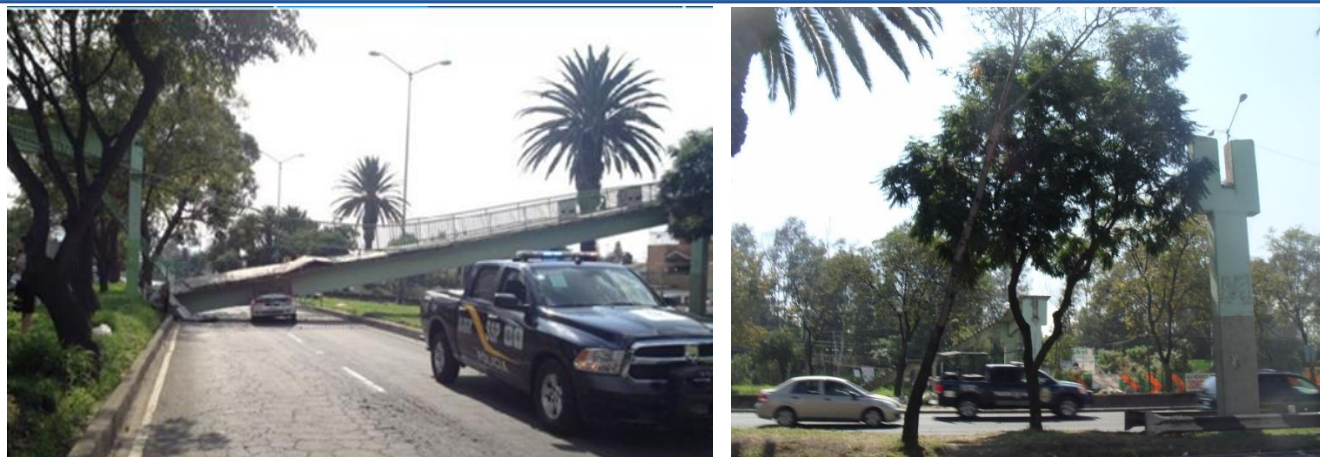


Fig. 94 Collapsed Pedestrian Overpass on Periferico Blvd

## CONCLUSIONS

The following conclusions can be drawn from the observations made by the CAEE reconnaissance team:

### Geoscience Aspects:

- The soft lacustrine clay in Mexico City tend to amplify ground motions over a broad period range varying between 1.0 and 5.0 sec. Unlike the 1985 Mexico City Earthquake, which caused widespread damage to long-period structures in the central portion of the city within Seismic Lake Sub-Zones IIIc and III d, the damage caused by the September 19, 2017 event was mostly in the transition zone (Seismic Zone II) and Seismic Lake Sub-Zones IIIa and IIIb.
- In the September 19, 2017 earthquake, the frequency content of the ground motion produced spectral peaks between 1.0 sec and 2.0 sec, affecting mid-rise buildings.
- While the problem of ongoing ground subsidence due to extraction of groundwater in the Mexico City is widely recognized for decades, the somewhat related problem of ongoing ground cracking and its intensification during seismic events, such as the September 19, 2017 event, has only recently been studied systematically since 2005.
- Intraplate events, being more frequent and often closer to major urban centres than their headline-grabbing major interplate counterparts, are receiving more attention with time. Mexican earthquake early-warning system began in the late 1980s, initially focusing on coastal interplate events. It has been improved and expanded to cover intraplate events, and has been available to serve the general public since 1993. Both Canada and USA are currently developing similar systems along the west coast; we look forward to further development of these systems.
- The earthquake early warning system implemented in Mexico functioned reasonably well due to frequent use since 1993. However, because the earthquake coincided with an anniversary of the 1985 Earthquake, it was mistaken by some for a drill, which might have reduced its effectiveness.
- The ongoing evolution of building code and related construction practice provide the public with earthquake protection commensurate with our up-to-date knowledge. Non-compliance of existing

structures with the current code is a difficult socio-economic issue. British Columbia has conducted a sustained program to upgrade school buildings for some time. This and other similar programs are important measures to remove and reduce the potential threat to life and property in the event of an earthquake.

- In seismically active areas, building renovations and seismic upgrades must be carried out by competent engineers/contractors, and inspected by regulators. Episodes of building partial and/or total collapse due to error, incompetence and other irregularities during this important phase are disheartening.
- Mexico City, with its frequent seismic events and unique subsoil conditions, and the ongoing structural deterioration of its building stock by repeated earthquake assaults, are both a concern and a tough issue to address. In some neighbourhoods, there are collapsed buildings sporadically distributed among similar buildings of same vintage, due to unfortunate combination of the given earthquake, site setting and structural make up.

Structural Aspects:

- Reinforced concrete frame buildings with masonry infill walls, confined masonry buildings and non-engineered traditional masonry and adobe buildings suffered the most damage during the September 19, 2017 Earthquake, especially if built prior to the improvements in seismic design practices following the 1985 Mexico City Earthquake.
- Lack of seismic design and detailing practices in older reinforced concrete columns and improper use of tie columns and bond beams in confined masonry, as well as non-compliant construction in general, were found to be the primary causes of damage, in addition to the ground motion amplification effects associated with prevailing soft soils conditions.
- Newer building built after the improvement of the Mexico City Seismic Code in the post-1985 era performed well. This is especially true in buildings built in more recent years. The lack of proper separation of masonry infill walls and their participation in seismic resistance resulted in varying degrees of masonry damage. This was observed to be also true in newer buildings.
- Lack of the implementation of current seismic code requirements for having proper separation between the buildings caused pounding effect, resulting in varying degrees of damage, sometimes causing partial or complete collapses.
- Soft-storey buildings performed poorly, especially if the soft storey columns did not have sufficient capacity to resist increased force and deformation demands.
- Retrofitted buildings performed well if the retrofit strategy involved cross bracing of frames, providing global drift control. However, the common form of column retrofit technique used in Mexico City, consisting of externally placed steel cages, made up of welded steel angles and steel strips, was not able to provide sufficient resistance to poorly designed columns.

- Comparison of seismic hazard values recorded after the earthquake with those used to design buildings in western Canada indicates that the buildings in Canada could be vulnerable to similar earthquakes if located on soft soils and not designed to have inelastic deformability.
- The unusual ground conditions of Mexico City, built on thick soft lake deposits, coupled with the widespread use of ground water for city's water needs resulted in extensive ground settlements before and during the earthquake. This resulted in the settlement, tilting and pounding of buildings with undesirable consequences.

### **Acknowledgement**

The technical information and assistance provided by the following individuals to the CAEE reconnaissance team are gratefully acknowledged:

- Jorge J. Jimenez Alcaraz of CDMX
- Carlos Humberto Huerta Carpizo, the National Autonomous University of Mexico
- Luciano Fernandez Sola of the Metropolitan Autonomous University
- Josué Garduño-Chávez, Universidad Nacional Autonoma de Mexico
- David Muria Vila of the National Autonomous University of Mexico
- Mark Yashinsky of the California Department of Transportation
- The Centro de Instrumentación y Registro Sísmico (CIRES)
- Alan Alonso Rivers, the University of Alberta
- Hector Manuel Toledo, the National Water Commission
- Mario Luna Antonio, Carso Group

### **References**

- Alberto, Y., Kyokawa, H., Otsubo, M., Kiyota, T. and Towhata, I. 2018. Reconnaissance of the 2017 Central Mexico Earthquake, JSCE Journal of Disaster FactSheets, FS2018-E-0001, <http://committees.jsce.or.jp/disaster/system/files/FS2018-E0001.pdf>
- Alcocer, S., Cesin, J., Flores, L.E., Hernandez, O. , Meli, R. , Tena, A. and Vasconcelos, D. (2003). The New Mexico City Building Code Requirements For Design and Construction of Masonry Structures. Proceedings, 9th North American masonry Conference, Clemson, South Carolina, U.S. June 1-4.
- Alcocer, S., Arias, J.G., and Vazquez, A. (2004<sup>a</sup>). Response Assessment of Mexican Confined Masonry Structures Through Shaking Table Tests, Proceedings of the 13th World Conference on Earthquake Engineering, Vancouver, Canada, Paper No. 2130.
- Anderson, J.G. et al. 1986. Strong Ground Motion from the Mochoacan, Mexico, Earthquake. Science, 233 (4768): 1043–9.
- Arroyo, D. et al. 2012. Evaluation of the change in dominant periods in the lake-bed zone of Mexico City produced by ground subsidence through the use of site amplification factors, <http://dx.doi.org/10.1016/j.soildyn.2012.08.009>.
- Atkinson, G.M. and Adams. J. 2013. Ground Motion Prediction Equations for Application to the 2015 Canadian National Seismic Hazard Maps, Can. J. Civ. Eng. 40, pp. 988-998.

- Benz, H.M. et al. 2011. Seismicity of the Earth - 1900–2010 Mexico and Vicinity, USGS Open-File Report 2010–1083-F, Revised ed. Boore, D. M. (2010). Orientation-independent, nongeometric-mean measures of seismic intensity from two horizontal components of motion, BSSA, 100(4), 1830-1835.
- Cruz VM, Krishna S, Ordaz M. Qué ocurrió el 19 de Septiembre de 2017 en México?. Mexico city (CDMX): Grupos de Sismología e Ingeniería de la UNAM; 2017. 9 p.
- Cuéllar, A. et al. 2014. The Mexican Seismic Alert System (SASMEX): Its alert signals, broadcast results and performance during the M 7.4 Punta Maldonado earthquake of March 20<sup>th</sup>, 2012. In Early Warning for Geological Disasters, pp. 71-87, Springer, Berlin, Heidelberg.
- Ernesto TT. Curso regional sobre diseño y construcción de estructuras de mampostería de acuerdo a las Normas NMX y MTC [Lecture notes]. Nuevo León: Sociedad Mexicana de Ingeniería Estructural, A.C.; 2014 [cited 2018 Jan 15]. Available from: <http://www.smie.org.mx/informacion-tecnica/>
- Ferrer H. Ingeniería sísmica [Lecture notes]. Puebla: Benemérita Universidad Autónoma de Puebla; 2013 [cited 2018 Jan 15].
- Galvis, F., Miranda, E., Heresi, P., Dávalos, H. and Silos, J.R. 2017. Preliminary Statistics of Collapsed Buildings in Mexico City in the September 19, 2017 Puebla-Morelos Earthquake, Oct. Stanford University, [https://www.researchgate.net/publication/320297374\\_Preliminary\\_Statistics\\_of\\_Collapsed\\_Buildings\\_in\\_Mexico\\_City\\_in\\_the\\_September\\_19\\_2017\\_Puebla-Morelos\\_Earthquake](https://www.researchgate.net/publication/320297374_Preliminary_Statistics_of_Collapsed_Buildings_in_Mexico_City_in_the_September_19_2017_Puebla-Morelos_Earthquake)
- García-Acosta, V. 2017. UNAM Report.
- García S. 2017 Observaciones ante emergencia geotécnica en algunas colonias de la delegación Tláhuac, CDMX Manifestaciones del suelo posteriores al sismo del 19 de septiembre de 2017, Instituto de Ingeniería UNAM.
- García-Acosta, V. and Suárez G. 1996. Los sismos en la historia de México, Vol. 1, Fondo de Cultura Económica (FCE)-Universidad Nacional Autónoma de México (UNAM)- Centro de Investigación y Estudios Superiores en Antropología Social (CIESAS), México, 718 pp.
- GEER 2018. Geotechnical Engineering Reconnaissance of the 19 September 2017 M<sub>w</sub> 7.1 Puebla-Mexico City Earthquake, GEER-055A Report, February 16.
- Giraldo S, Arredondo C, Reinoso E. ¿Está contemplado el sismo del 19 de Septiembre de 2017 en nuestros reglamentos?. Mexico city (CDMX): ERNtérate Nota de interés. 2017. 1p. Available from: <https://ern.com.mx/web/sismo19S.html?v.1.17>
- Guevara T. “Soft Story” and “Weak Story” in earthquake resistant design: A multidisciplinary approach. Lisboa: 15th World Conference on Earthquake Engineering. 2012. 10p. Available from: [http://www.iitk.ac.in/nicee/wcee/fifteenth\\_conf\\_purtgal/](http://www.iitk.ac.in/nicee/wcee/fifteenth_conf_purtgal/)
- II.UNAM 2017a. The Subsoil of Mexico City, Vols. I and II Parts A to D Marsal, R.J. and Mazari, M. Vol. III Parts E to G Auvinet, G., Mendez, E. and Juarez, M, Instituto de Ingeniería, UNAM.
- II.UNAM 2017b. Reporte Preliminar del Sismo del 19 de Septiembre de 2017, [in Spanish], Instituto de Ingeniería, UNAM.
- Lesser J.M. and Cortés M. 1998. El hundimiento del terreno en la ciudad de Mexico y sus implicaciones en el Sistema de drenaje. Ingeniería Hidráulica en Mexico; 3(13): 13–8.
- Lo, R.C. and Yniesta, S. 2019. Geoscience Aspect of September 19, 2017 Mexico Puebla-Morelos Earthquake, Proc. 12<sup>th</sup> CCEE, Quebec City, June.

- Manica MA. Comportamiento dinámico de inclusiones rígidas [Master's thesis]. Mexico city (CDMX): National University Autonomous of Mexico; 2013. 156 p.
- Mayoral, J.M., E. Castañón, L. Alcántara, S. Tepalcapa. (2016). Seismic response characterization of high plasticity clays. *Soil Dynamics and Earthquake Engineering*, Elsevier, 84, 174-189.
- Meli R. Comentarios y ejemplos de las normas técnicas complementarias para diseño y construcción de estructuras de mampostería, DDF [Internet]. Mexico city: Instituto de Ingeniería de la UNAM; 1992 [cited 2018 Jan 15]. 115 p. Available from: <https://aplicaciones.iingen.unam.mx/ConsultasSPII/Buscarnpublicacion.aspx>
- Mitchell, D., Adams, J., DeVall, R.N., Lo, R.C., and Weichert, D. 1986. Lessons from the 1985 Mexican Earthquake, *Can. J. Civ. Eng.* 13, pp. 535-557.
- Nakamura, Y. 1989. A method for dynamic characteristics estimation of subsurface using microtremor on the ground surface, *Q. Rep. Railway Tech. Res. Inst.* 30, 25–30.
- NBCC-2015. National Building Code of Canada, NRC, 2015.
- Normas Técnicas Complementarias para Diseño por Sismo (NTC-DS), 2004 (in Spanish), Gobierno del Distrito Federal, Mexico City.
- NTCS-04 2004. *Normas Técnicas Complementarias para diseño por sismo*, Gaceta oficial del Distrito Federal, México.
- Reglamento de Construcciones para el Distrito Federal (RC-DF), 2004 (in Spanish), Gobierno del Distrito Federal, Mexico City or Mexico City Building Code (MCBC).
- Ordaz, M. and Singh, S. K. 1992. Source spectra and spectral attenuation of seismic waves from Mexican earthquakes, and evidence of amplification in the hill zone of Mexico City. *BSSA*, 82(1), 24-43.
- Ordazi, M. and Meli, R. 2004. Seismic design and codes in Mexico. *Proceedings of the 13<sup>th</sup> World Conference on Earthquake Engineering*, Paper No. 4000. Vancouver, BC.
- Post, N. M. 2017. Lessons from the Sept. 19 Mexico Earthquake, *Engineering News-Record*, Oct. 18. <https://www.enr.com/articles/43128-lessons-from-the-sept-19-mexico-ea>.
- Rathje, E. M. et al. 1998. Simplified frequency content estimates of earthquake ground motions. *Journal of Geotechnical and Geoenvironmental Engineering*, 124(2), 150-159.
- Reinoso E. Aspectos sismológicos y efectos de los sismos del 7 y 19 de Septiembre del 2017. [Lecture notes]. Mexico city (CDMX): Sociedad Mexicana de Ingeniería Estructural, A.C.; 2017 [cited 2018 Jan 15]. Available from: <http://www.smie.org.mx/informacion-tecnica/>
- Rosenblueth E, García V, Rojas T, Nuñez FJ, Orozco J. Macrosismos [Internet]. Mexico city (CDMX): Impresores cuadratín y medio; 1992 [cited 2018 Jan 15]. 27 p.
- Saatcioglu, M. et al. 2019. Performance of Structures during the September 19, 2017 Puebla Morelos Earthquake in Mexico, *Proc. 12<sup>th</sup> CCEE*, Quebec City, June.
- Sabloff, J.A. 1997. *The Cities of Ancient Mexico – Reconstructing a Lost World*, Thames and Hudson.
- SEAOSC 2017. Safer Cities Recon – Mexico City EQ – Trip Summary, Oct. 30. <https://www.seaosc.org/Safer-Cities-Recon/5456992>
- Singh, J. P. 1985. Earthquake Ground Motions: Implications for Designing Structures and Reconciling Structural Damage, *Earthquake Spectra*, Vol. 1, No. 2, pp. 239-270.

- Singh, S.K. et al. 2015. Intraslab versus Interplate Earthquakes as Recorded in Mexico City: Implications for Seismic Hazard, *Earthquake Spectra*, Vol. 31, No.2, pp. 795-812.
- Singh, S. K. et al. 1999. A Preliminary report on the Tehuacan, Mexico earthquake of June 15, 1999 (Mw= 7.0), *Seismological Research Letters*, 70(5), 489–504.
- Singh, S. K. et al. 1996. The great Mexican earthquake of 19 June 1858: Expected Ground Motions and Damage in Mexico City from a Similar Future Event, *BSSA*, 86(6), 1655–1666.
- Soto H. Causas preliminares de los daños por el sismo. *Revista mexicana de la construcción* [Internet]. 2017 Nov [cited 2018 Jan 15]; 630: 26-32. Available from: <http://www.cmic.org.mx/rmc/>
- Suter, M. et al. 1996. Macroseismic Study of Shallow Earthquakes in the Central and Eastern Parts of the Trans-Mexican Volcanic Belt, Mexico, *BSSA*, Vol. 86(6), pp. 1952-1963.
- Team work from Servicio Sismológico Nacional, UNAM. Sismo de Tehuantepec (2017-09-07 23:49 M8.2). Mexico city: Servicio Sismológico Nacional; 2017. 11 p. Available from: <http://www2.ssn.unam.mx:8080/catalogo/>
- UNAM 2018. [www.repsa.unam.mx/documentos/Cuenca-Lagos.kmz](http://www.repsa.unam.mx/documentos/Cuenca-Lagos.kmz).
- USGS 2018a. <https://earthquake.usgs.gov/earthquakes/eventpage/us2000ahv0#executive>. searched in 2018.
- USGS 2018b. <https://earthquake.usgs.gov/archive/product/poster/20170919/us/1506025242898/poster.pdf>. searched in 2018.
- Valenzuela-Beltrán, F. et al. 2017. On the Seismic Design of Structures with Tilting Located within a Seismic Region, *Appl. Sci.* 7, 1146; doi:10.3390/app7111146.  
[www.repsa.unam.mx/documentos/Cuenca-Lagos.kmz](http://www.repsa.unam.mx/documentos/Cuenca-Lagos.kmz) [Last accessed November 16<sup>th</sup> 2017]
- Yniesta, S. 2019. Ground Response in the September 19<sup>th</sup> 2017 M<sub>w</sub> = 7.1 Central Mexico Earthquake, Paper to be submitted to 7<sup>th</sup> International Conference on Earthquake Geotechnical Engineering, Rome, Italy.
- Zeevaert, L. and Newmark, N. M. 1956. Aseismic design of Latinoamericana Tower in Mexico City, *Proc. of WCEE*, Berkeley, CA, pp. 35-1 - 35-11.
- Zeevaert, L. 1982. *Foundation Engineering for Difficult Subsoil Conditions*, 2<sup>nd</sup> edition, Van Nostrand Reinhold, New York.